Department of Radio Science and Engineering

Spherical wave theory applied to mobile radio channel modeling, synthesis and emulation

Afroza Khatun

Aalto University

DOCTORAL DISSERTATIONS

Aalto University publication series
DOCTORAL DISSERTATIONS 205/2014

Spherical wave theory applied to mobile radio channel modeling, synthesis and emulation

Afroza Khatun

A doctoral dissertation completed for the degree of Doctor of Science (Technology) to be defended, with the permission of the Aalto University School of Electrical Engineering, at a public examination held at the lecture hall S3 of the school on 12 December 2014 at 12.

Aalto University
School of Electrical Engineering
Department of Radio Science and Engineering

Supervising professors
Prof. Pertti Vainikainen, until June 30, 2012
Prof. Keijo Nikoskinen, as of November, 2012

Thesis advisors
D.Sc. (Tech.) Tommi Laitinen
D.Sc. (Tech.) Veli-Matti Kolmonen
Assist. Prof. Katsuyuki Haneda

Preliminary examiners
Dr. Wim Kotterman, Ilmenau University of Technology, Germany
Dr. Jon W. Wallace, Wavetronix, Provo, UT, USA

Opponent
Prof. Alain Sibille, Telecom ParisTech, France

Aalto University publication series
DOCTORAL DISSERTATIONS 205/2014

ISBN 978-952-60-6009-5 (printed)
ISBN 978-952-60-6010-1 (pdf)
ISSN-L 1799-4934
ISSN 1799-4934 (printed)
ISSN 1799-4942 (pdf)
http://urn.fi/URN:ISBN:978-952-60-6010-1

Unigrafia Oy
Helsinki 2014

Finland

441 697
Printed matter

Aalto University

Abstract

Aalto University, P.O. Box 11000, FI-00076 Aalto www.aalto.fi

Author
Afroza Khatun

Name of the doctoral dissertation
Spherical wave theory applied to mobile radio channel modeling, synthesis and emulation

Publisher School of Electrical Engineering

Unit Department of Radio Science and Engineering

Series Aalto University publication series DOCTORAL DISSERTATIONS 205/2014

Field of research Radio Engineering

Manuscript submitted 9 June 2014 **Date of the defence** 12 December 2014

Permission to publish granted (date) 7 November 2014 **Language** English

☐ **Monograph** ☒ **Article dissertation (summary + original articles)**

Abstract

The future mobile communication systems will provide increasing data rates to satisfy the service requirements of the users. This means that the radio performance of especially the mobile terminals becomes more important and has to be as good as possible. Thus, it is very important to be able to evaluate the performance of the antennas of the mobile terminals in a realistic way. This thesis deals with practical and theoretically justified ways to describe both the field environment and the radiated fields of mobile terminal antennas and antenna systems using spherical wave theory. In this thesis, advanced measurement methods that facilitate the radio wave propagation channel as well as mobile terminal antenna characterization are developed.

The research in this thesis contributes to three key areas: (1) channel-independent antenna characterization and performance assessment, (2) degrees-of-freedom (DoF) of propagation channels and (3) over-the-air (OTA) testing. In the first part of this thesis, theoretical considerations of the spherical wave expansion (SWE) for the antenna array configuration on the cubical surface for estimating the propagation channel and measuring the antenna radiation through a near-field to far-field transformation (NF-FF) are studied. A novel technique, azimuthal mode decomposition (AMD) for the reduction of the computational burden is presented for both applications using the cubical array configuration.

In second part, the proposed antenna configuration is applied to the estimation of the degrees of freedom (DoF) in spatial multipath channels. In multi-antenna systems, such as multiple-input multiple-output (MIMO), multiple-input single-output (MISO), this DoF provides the number of antenna elements on the aperture for efficiency improvement of the system performance by utilizing the spatial transmission, e.g., diversity and multiplexing.

In the third part of this thesis, multi-probe based MIMO over-the-air (OTA) testing is described for the performance evaluation of multi-antenna systems. The related uncertainties of such testing, for instance, the required number of probes, optimum probe placement and the influence of the probe polarization are investigated in theory and practice.

Keywords Radio channel, MIMO, spherical wave expansion, antenna array, field synthesis, near-field measurement, OTA testing.

ISBN (printed) 978-952-60-6009-5 **ISBN (pdf)** 978-952-60-6010-1

ISSN-L 1799-4934 **ISSN (printed)** 1799-4934 **ISSN (pdf)** 1799-4942

Location of publisher Helsinki **Location of printing** Helsinki **Year** 2014

Pages 147 **urn** http://urn.fi/URN:ISBN:978-952-60-6010-1

Preface

This thesis work has been carried out during June 2009 – March 2014 at the Department of Radio Science and Engineering in Aalto University School of Electrical Engineering. For the financial support, I thank the Academy of Finland, the Japan Society for the Promotion of Science, the Centre of Excellence in Smart Radios and Wireless Research – SMARAD, the Finnish Funding Agency for Technology and Innovation (TEKES), Finnish telecommunication industry and Nokia Foundation.

I am grateful to my first supervisor, the late Professor Pertti Vainikainen for accepting me as one of his doctoral students and giving me the opportunity to work on this interesting and challenging field. Professor Keijo Nikoskinen deserves warm thanks as well, for helping me through the fruitful discussions and guidance in the final phase of the thesis. I would like to express my deepest gratitude to my instructors Dr. Tommi Laitinen, Dr. Veli-Matti Kolmonen, and Assistant Professor Katsuyuki Haneda for their invaluable guidance, extensive discussions, co-operation, encouragement, useful support at every stage of this work. In addition, I wish to acknowledge all of the other co-authors of my publications for their significant contributions to this thesis. Especial thanks go to Mr. Pekka Kyösti for his co-operation and useful support to this thesis.

I would like to thank the pre-examiners of my thesis, Dr. Jon Wallace and Dr. Wim Kotterman for their reviews and valuable comments to improve the quality of the thesis.

I would like to thank the whole personnel in the Department of Radio Science and Engineering for the nice working atmosphere. Especially I would like to mention Annakaisa, Azremi, Janne, Jan, Usman, Sathya, Zhou, Suzan, Suiyan, Martta, Mina, Lorenz, Dr. Timo, Dr. Clemens, Stina, Tuula, Sari and Mirjum. My warm thanks go to all of my Bangladeshi friends in Finland for sharing the enjoyable moments and encouragement during the study period.

I owe my loving thanks to my parents, Md. Aftab Uddin and Halima Khatun, my parents-in-law, Md. Abdul Khaleque and Roksana Parvin, my siblings Tonnee and Tuhin, and other family members for their love, encouragement, support and prayers. Despite of the distance, I feel from the bottom of my heart as if they were always beside me and that facts encourage me to all the aspects of success in my life. My deepest and most heartfelt thanks belong to my loving and caring husband, *Dristy Parveg* for his strong support, patience, love, inspiration and encouragement through all of the period. It would not have been possible to write this doctoral thesis without you.

Finally, all of my gratitude would be definitely incompleted if I would forget to thanks the most merciful and gracious ALLAH.

Espoo, November 23, 2014

Afroza Khatun

Contents

List of Publications

This doctoral dissertation consists of a summary and of the following publications which are referred to in the text by their numerals

[I] A. Khatun, T. Laitinen, and P. Vainikainen, "Spherical wave modelling of radio channels using linear scanners," In *Proceedings of the 4th European Conference on Antennas and Propagation (EuCAP 2010)*, Barcelona, Spain, 5 pages, 12-16 April 2010

[II] A. Khatun, T. Laitinen, and P. Vainikainen, "Azimuthal mode decomposition technique for cubical surface scanning with the application to spherical mode field synthesis," *IEEE Antennas and Wireless Propagation Letters,* vol. 12, pp. 1196-1199, 2013.

[III] A. Khatun, T. Laitinen, and P. Vainikainen, "Cubical surface scanning for near-field antenna measurements using spherical wave expansion," *Antenna Measurement Techniques Association*, *33rd Annual Meeting & Symposium (AMTA 2011),* Denver, CO, USA 2011, pp. 16-21.

[IV] K. Haneda, A. Khatun, M. Dashti, T. Laitinen,V.-M. Kolmonen, J.-i. Takada, and P. Vainikainen, "Measurement-based analysis of spatial degrees-of-freedom in multipath propagation channels," *IEEE Transaction on* Antennas *and Propagation,* vol. 61, no. 2, pp. 890-900, Feb. 2013.

[V] A. Khatun, T. Laitinen, V.-M. Kolmonen, and P. Vainikainen, "Dependence of error level on the number of probes in over-the-air multiprobe test systems," *International Journal of Antennas and Propagation,* volume 2012, Article ID 624174, 6 pages, 2012.

[VI] A. Khatun, V.-M. Kolmonen, T. Laitinen, and K. Nikoskinen, "Clarification of uncertainties in MIMO over-the-air multi-probe test systems," In *Proceedings of the 7th European Conference on Antennas and Propagation (EuCAP 2013),* Gothenburg, Sweden, pp. 1427-1431, 8-12 April 2013.

[VII] P. Kyösti and A. Khatun, "Probe configurations for 3D MIMO over-the-air testing," In *Proceedings of the 7th European Conference on Antennas and Propagation (EuCAP 2013),* Gothenburg, Sweden, pp. 1421-1425, 8-12 April 2013.

[VIII] A. Khatun, V.-M. Kolmonen, D. Parveg, V. Hovinen, M. Berg, K. Haneda, K. Nikoskinen, and E. Salonen, "Multi-probe based MIMO over-the-air testing with plane-wave field synthesis," *IEEE Transaction on Antennas and Propagation (submitted).*

Author's Contribution

The author has the main contribution to all the publications where she is listed as the first author ([**I**], [**II**], [**III**], [**V**],[**VI**], [**VIII**]). The author has a significant contribution to the other publications ([**IV**], [**VII**]).

[**I**] The author had main responsibility for developing the idea. The author carried out all the formulations, performed the simulations, and was responsible for writing the publication. Dr. Tommi Laitinen participated in the development of the idea and in the writing of the paper.

[**II**] The method was proposed by Dr. Tommi Laitinen. The author was responsible for developing the method and carried out the simulations. She was the responsible for writing the publication.

[**III**] The author had main responsibility for developing the idea. The author carried out the simulations and was responsible for writing the publication. The work was instructed by Dr. Tommi Laitinen.

[**IV**] The author participated to the measurement, writing the paper and data analysis. Assistant Prof. Katsuyuki Haneda had the leading role in preparing the paper.

[**V**] The author had main responsibility for writing the manuscript and data analysis. Dr. Tommi Laitinen and Dr. Veli-Matti Kolmonen participated in writing of the publication.

[**VI**] The author had the leading role in the work. The author carried out the simulations and was responsible for writing the publication. Dr. Veli-Matti Kolmonen participated in the simulations.

[**VII**] The concept is a joint effort between Pekka Kyösti and the author. The author participated in simulations and writing the paper. Pekka Kyösti had the leading role in preparing the paper.

[**VIII**] The author had the main responsibility for developing the simulation tool, writing the paper, planning the measurement, and analyzing the measured data. Dr. Veli-Matti Kolmonen participated in developing the simulation tool. Prof. Katsuyuki Haneda and Dr. Veli-Matti Kolmonen participated in writing the paper.

List of Abbreviations

1G	First generation
2D	Two dimensional
2G	Second generation
3D	Three dimensional
3G	Third generation
3GPP	3rd Generation partnership project
4G	Fourth generation
AMD	Azimuthal mode decomposition
AoA	Angle of arrival
AoD	Angle of departure
APS	Angular power spectrum
ASA	Angular spread of arrival
ASD	Angular spread of departure
BS	Base station
CDMA	Code division multiple access
CQI	Channel quality indicator
CTIA	Cellular telecommunications industry association
DoF	Degrees of freedom
DUT	Device under test
e.g.	for example
FoM	Figure of merit
GSM	Global system for mobile communications
i.e.	that is
LOS	Line-of-sight
LTE	Long term evolution
LTE-A	Long term evolution advanced

MIMO	Multiple-input multiple-output
MISO	Multiple-input single-output
NF-FF	Near-field to far-Field
NLOS	Non-line-of-sight
OTA	Over-the-air
PAS	Power azimuth spectrum
PES	Power elevation spectrum
PFS	Prefaded signal synthesis
PWS	Plane wave field synthesis
RF	Radio frequency
Rx	Receiver
SCM	Spatial channel model
SISO	Single-input single-output
SWE	Spherical wave expansion
TRP	Total radiated power
TRS	Total radiated sensitivity
Tx	Transmitter
TDMA	Time division multiple access
UE	User equipment

List of Symbols

a	length of the side of the cube
$\bar{a}$	inward-propagating spherical modes, vector
$\bar{a}_r, \bar{a}_\theta, \bar{a}_\varphi$	unit vector
c	index of radial dependence of the spherical wave functions
$\bar{C}_m$	azimuthal mode coefficients
d_s, d_u	distances
D	DoF of propagation channel
$\bar{E}$, $\bar{E}_0$, $\bar{E}_1$, $\bar{E}_2$, $\bar{E}_3$	electric field vectors
$\bar{E}_{syn\_no,j}$	synthesis field vector
$\bar{E}_{tar,j}$, $\bar{E}^0_{tar,j}$,$\bar{E}^0_{tar,j}$,$\bar{E}^0_{tar,j}$,$\bar{E}^0_{tar,j}$	target electric field vector
$\bar{\bar{E}}_C$, $\bar{\bar{E}}_0$, $\bar{\bar{E}}_1$, $\bar{\bar{E}}_2$, $\bar{\bar{E}}_3$, $\bar{\bar{F}}$	coupling matrices
$\bar{F}^{(c)}_{smn}$	spherical vector wave function
$\bar{\bar{F}}$	spherical vector wave function matrix
F_{rx}, F_{tx}	radiation pattern
$\bar{\bar{H}}$, $\bar{H}$	transfer functions
i	imaginary unit
j, l, s, u	indices
J	number of spherical modes
k	wave number
k_0, K, L,L_{k_0}, n_1, N_1, N_C, N_T, N_t, N_r,T	numbers
M	truncation number for the m index of the spherical wave expansion
$\bar{\bar{M}}$	spherical-mode to spherical-mode channel matrix
N	truncation number of spherical wave mode

	series
$\bar{P}_n^{\lvert m \rvert}$	normalized associate Legendre functions
Q, $Q_{smn}^{(c)}$	spherical wave coefficients
$\bar{Q}$, $\bar{Q}_j$	spherical wave coefficients vectors
r_0	radius of a minimum sphere
r	radius
$\bar{r}$	mode coupling vector
r_j	mode response of channel
$\bar{\bar{R}}$	antenna receiving coefficient matrix
$\bar{\bar{r}}_r$	correlation matrix
s, m, n	spherical mode indices
$\bar{\bar{T}}$	antenna transmitting coefficient matrix
$\bar{x}_j$	spherical mode input signal
$\bar{x}$	input signal vector
x	coordinate
y	coordinate
y_r	receive signal
$\bar{y}_r$	receive signal vector
z	coordinate
$z_n^{(c)}$	radial spherical wave function
α	polarimetric path gain
δ_0	dirac delta function
δ	Kronecker delta
ϵ	free-space permittivity
ϵ_t, ϵ_n	maximum amplitude error
η_0	free-space field impedance
θ	elevation angle in the spherical coordinate
λ	wavelength
μ	free-space permeability
ν	Doppler shift
ξ	white Gaussian noise
$\bar{\xi}$	white Gaussian noise vector
π	constant
ρ	noise amplitude

τ	delay
φ	azimuth angle in the spherical coordinate
ϕ	azimuth angle of departure
ψ	azimuth angle of arrival
ω	angular frequency

1. Introduction

1.1 Scope

The evolution of cellular wireless mobile networks can be discretely grouped into various generations. The first generation (1G) networks introduced in the 1980's were represented by an analog wireless access system primarily for voice traffic [1]. These networks were then superseded by digital second generation (2G) networks. Third generation (3G) networks were a significant leap over 2G developed in early 1990's, providing much higher data rates, significant increase in voice capacity, and supporting advanced services and applications, including multimedia. With the success of 2G and 3G, recently fourth generation (4G) wireless networks have been introduced to meet the increased consumer demand on high data rate applications—such as music and video downloading, web browsing, and multimedia sharing.

In mobile communications, the antennas on mobile terminals are an indispensable part of the system. They can be considered as transition devices between guided waves and free space waves and play an important role to determine the system performance for a particular propagation channel in which the antennas operate. Thus, it is very important to be able to evaluate the performance of the antennas of the mobile terminals in a realistic way. Furthermore, it is essential to understand the coupling between the antennas and the propagation channel comprehensively to optimize the antenna performance in the environment and thus maximize the system performance. Therefore, theoretical and practical investigations in antenna design as well as in radio channel modeling are drawing the considerable attention of researchers. As a consequence both antenna and channel measurements take a central part in mobile communications.

Today, near-field scanning over canonical geometries – planar, cylindrical, and spherical – is extensively used for determining the antenna far-field

pattern together with near-field to far-field (NF-FF) transformation algorithms [2]. Apart from these, techniques for more special scanning geometries, e.g., plane-polar, plane-bi-polar etc. have been developed [3-4]. Scanning can also be performed for synthesizing fields using the virtual array principle. For example, an approach to the spherical wave modeling of radio channels has been proposed in [5] and here the field synthesis becomes useful in finding the spherical mode field responses of the radio propagation channel.

The 4G wireless radio technologies such as the long term evolution (LTE), long term evolution advanced (LTE-A) and worldwide interoperability for microwave access (WiMAX) have introduced multiple-input multiple-output (MIMO) technique in order to improve wireless network performance in terms of data throughput and reliability [6-7]. The MIMO technique involving multiple antennas at both terminals supports performance-enhancing techniques such as spatial multiplexing, beam forming, and spatial diversity [8-10]. The MIMO performance in a multi-antenna communication system depends on the spatial features of the propagation channel and on how much of the available degrees of freedom (DoF) in the channel can effectively be exploited. This is heavily influenced by the construction of the terminal, especially with respect to the placement of the antenna elements [11-13]. Over-the-air (OTA) testing is one widely used method of evaluating the terminal antenna performance. It is able to take into account the antenna and device characteristics, and radio propagation conditions in some extent [14-16]. However, it is important for such so-called MIMO OTA test systems that they are capable of synthesizing an electromagnetic environment, which realistically represents the environment where the device operates. One possible way to synthesize radio channel environments is through the exploitation of multi-probe technology [17-20].

1.2 Objectives and contents

The goal of this thesis is to find practical and theoretically justified ways to describe both the field environment of the propagation channel and the radiated fields of mobile terminal antennas and antenna systems using the spherical wave theory. In this thesis, advanced measurement methods that facilitate the radio wave propagation channel as well as mobile terminal antenna characterization are developed.

The main scientific results of this thesis are presented in publications [**I-VIII**]. The contribution of this thesis to the research field can be divided into

three parts. The first part of the thesis concerns on the channel-independent antenna characterization and performance assessment with spherical wave decompositions [**I**–**III**]. In the second part, the DoF of the propagation channel is reported, where a novel aspect of computing DoF from spherical wave decomposition is considered [**IV**]. The third part focuses on the multi-probe based OTA testing for MIMO antenna performance evaluations [**V**–**VIII**].

In this thesis, the main results are summarized into a large scientific context. The summary is organized as follows. Chapter 2 gives a short introduction to the theoretical background of the spherical wave expansion (SWE), which is extensively used in this thesis. Chapter 3 focuses on measurement method applied to radio channel modeling and near-field antenna measurements. A novel type of a measurement method is reported for both purposes. The experimental validation of the method is studied in Chapter 4. Importantly, a novel method for the estimation of the DoF of the propagation channel is reported in Chapter 4. In Chapter 5, synthesis and emulation of realistic radio channels in anechoic environments for OTA testing of multi-antenna mobile handsets is analyzed. A summary of the publications consisting this thesis is presented in Chapter 6. Finally, the conclusions and possible ideas for future research are given in Chapter 7.

2. Spherical wave expansion

The results of this thesis are based on the spherical wave theory applied for characterizing both the field environment of the propagation channel and the radiated fields of mobile terminal antennas. This relevant theory, which is based on the use of the SWE [21] constituting a set of orthogonal basis functions in spherical coordinates, will be presented in this chapter. In this thesis, SWE is used as a theoretical basis for analyzing the radiated fields. All radiated fields are assumed time-harmonic.

The antennas and propagation channel described by means of the electromagnetic field can be expressed in terms of the truncated series of the SWE. Due to the cut-off property of spherical wave series, the number of terms in such truncated SWE is controllable and only depends on the antenna dimension radiating in a propagation environment. This SWE has been applied widely in spherical antenna measurements, e.g., in [21]. The notations of the SWE used in this chapter of the thesis are similar to that of [21]. The time dependence of the electromagnetic fields assumed in this thesis is $e^{-i\omega t}$, where ω is the angular frequency of a radio-frequency (RF) signal. The electric field in a source-free region of space can be written as a weighted sum of the spherical wave function as

$$\bar{E}(r,\theta,\varphi) = k\sqrt{\eta_0}\sum_{s=1}^{2}\sum_{n=1}^{\infty}\sum_{m=-n}^{n} Q_{smn}^{(c)}\,\bar{F}_{smn}^{(c)}(r,\theta,\varphi), \tag{2.1}$$

where $\bar{E}(r,\theta,\varphi)$ is the electric field in standard spherical coordinates (r,θ,φ); k is the wave number; $\eta_0 = \sqrt{\mu/\epsilon}$ is the free-space field impedance; s, m and n are the spherical mode indices; $Q_{smn}^{(c)}$ are the spherical vector wave coefficients; and $\bar{F}_{smn}^{(c)}(r,\theta,\varphi)$ represent the power normalized spherical vector wave functions in spherical coordinates. It is known that the $\bar{F}_{smn}^{(c)}(r,\theta,\varphi)$ functions

are separated into radial, elevation and azimuth functions, where the radial functions are specified by the upper index c, the elevation functions are the Associate Legendre functions and the azimuth functions are the exponential functions. Index n represents the degree of the radial function, index m is the index for the azimuth function and values of $s = 1$ and 2, represent the transverse electric and the transverse magnetic field. The functions $\bar{F}_{smn}^{(c)}(r, \theta, \varphi)$ are defined as

$$\bar{F}_{1mn}^{(c)} = p_{mn}\left\{z_n^{(c)}(kr)\frac{im\bar{P}_n^{|m|}(cos\theta)}{sin\theta}\bar{a}_\theta + z_n^{(c)}(kr)\frac{\mathrm{d}\bar{P}_n^{|m|}(cos\theta)}{\mathrm{d}\theta}\bar{a}_\varphi\right\} \tag{2.2}$$

and

$$\bar{F}_{2mn}^{(c)} = p_{mn}\left\{\frac{n(n+1)}{kr}z_n^{(c)}(kr)\bar{P}_n^{|m|}(cos\theta)\bar{a}_r + \frac{1}{kr}\frac{\left(krz_n^{(c)}(kr)\right)}{\mathrm{d}(kr)}\frac{\mathrm{d}\bar{P}_n^{|m|}(cos\theta)}{\mathrm{d}\theta}\bar{a}_\theta + \frac{1}{kr}\frac{(krz_n^{(c)}(kr))}{\mathrm{d}(kr)}\frac{im\bar{P}_n^{|m|}(cos\theta)}{sin\theta}\bar{a}_\varphi\right\}, \tag{2.3}$$

with

$$p_{mn} = \frac{1}{\sqrt{2\pi}}\frac{1}{\sqrt{n(n+1)}}\left(-\frac{m}{|m|}\right)^m e^{im\varphi}, \tag{2.4}$$

where $\bar{P}_n^{|m|}(\cdot)$ is the normalized Associate Legendre function as defined by Belousov [22]. The radial function $z_n^{(c)}(kr)$ is one of the functions

$z_n^{(1)}$, spherical Bessel function

$z_n^{(2)}$, spherical Neumann function

$z_n^{(3)}$, spherical Hankel function of the first kind

$z_n^{(4)}$, spherical Hankel function of the second kind

where $c = 1$ and 2 correspond to radial standing waves, finite or infinite at the origin, respectively, whereas $c = 3$ and 4 correspond to radial outgoing and incoming waves, respectively. Due to the well-known cut-off property of the spherical wave functions, the expansion in (2.1) can be truncated appropriately at a finite $n = N$, where the truncation number is

$$N = [kr_0 + n_1]. \tag{2.5}$$

Hence, the expansion of the electromagnetic field with the truncated series of spherical wave functions becomes

$$\bar{E}(r,\theta,\varphi) = k\sqrt{\eta_0}\sum_{s=1}^{2}\sum_{n=1}^{N}\sum_{m=-n}^{n} Q_{smn}^{(c)}\,\bar{F}_{smn}^{(c)}(r,\theta,\varphi). \tag{2.6}$$

In (2.5), r_0 is the radius of the minimum sphere that fully encloses the device, n_1 is a small integer number, and the square brackets indicate the nearest integer number greater than or equal to the number inside the brackets. Typically, n_1 varies from $n_1 = 0$ to 10 [21] depending on the desired accuracy of the field characterization. For electrically relatively small antennas, for instance, antennas with $r_0 < 2\lambda$, a clearly smaller value, e.g., $n_1 = 2$ can be applied [23]. λ is the wavelength of the carrier frequency. The spherical wave mode, indicated by index j is calculated from $j = 2(n(n+1) + m - 1) + s$ and the total number of modes in the spherical wave characterization is $J = 2N(N+2)$.

3. Method for radio channel and near-field antenna measurements: cubical surface scanning

The MIMO systems have attracted much attention from the late 90's [11, 24-25], which utilize multiple antennas at both ends of the communication link. They exploit spatial information of radio wave propagation and have the potential to provide significant improvement in system performance in terms of, e.g., link reliability and data rates. An illustration of the elements of the MIMO link, i.e., antenna arrays at both terminals and propagation paths, is shown in Figure 3.1. The N_t and N_r are the number of antenna elements at the transmitter (Tx) and receiver (Rx), respectively. The propagation channel describes the behavior of the electromagnetic fields, which is antenna independent whereas the radio channel describes the channel responses including the antenna effect and propagation channel.

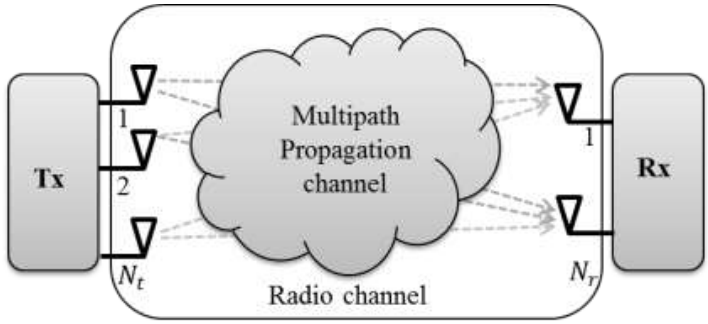

Figure 3.1. The MIMO link.

In MIMO systems, the antennas are fundamental elements and play an essential role in maximizing system performance for a given propagation channel. Therefore, comprehensive understanding of the phenomena of

interaction between the antennas and the propagation channel is essential for analyzing and optimizing the system performance. To study the antenna-channel interaction, [26] introduced the double directional channel model that describes the angle of departure (AoD) and angle of arrival (AoA) of the propagation paths.

The most common approach to consider the realistic propagation phenomena for the evaluation of wireless systems is the use of channel models, e.g., [27-35]. The conventional channel models have been constructed based on many measurement campaigns, but in most cases, the number of measurement samples has been insufficient of modeling every possible propagation scenario. Another critical issue in the channel modeling research is the limitation of the channel modeling method. The majority of the methodologies for the modeling and calculation of the coupling of the electromagnetic signals from the channel to the terminal are typically based on the multipath components or plane waves [26-35]. In the plane-wave, based modeling an assumption is made that the signal at the terminal is a superposition of a finite number of plane waves arriving at the terminal. However, in indoor scenarios, in particular, this underlying assumption for representing the signal at the terminal may not be very concise. In such scenarios, the dense multipath components are present which consist of diffuse or random scattering that causes weak and possibly very densely located multipath components and hence, it is relevant to consider the channel as a general near-field channel. This thesis, instead of traditional plane-wave and far-field based modeling, concentrates alternatively on the spherical-wave modeling of the electromagnetic environment created by the propagation channels and considers more general conditions of the channel without assuming a fixed number of plane waves.

The basis of the spherical-wave modeling is presented in Chapter 2. The well-known empirical relation (2.5) between the geometrical dimensions of the antenna and the highest index of the radial spherical wave modes can be used to increase the accuracy of the field characterization and computational efficiency. Furthermore, compared with widely used plane-wave methods, the proposed approach provides data reduction due to the orthogonal properties of the spherical harmonics and the compactness of the field characterization. Thus, the spherical-wave modeling becomes an attractive, new opportunity for propagation channel modeling.

In spherical-wave modeling, the idea is to consider the responses of the radio channel for different spherical wave mode fields. This chapter describes how the required spherical mode responses of a channel can be extracted from the

measurement data acquired on a cubical scanning surface. Firstly, Section 3.1 introduces the double directional channel models for MIMO link in free space. The multimode representation of the channels is presented in Section 3.2. Section 3.3 discusses the method of calculating the required spherical mode responses of the channel from data acquired using cubical scanning. Furthermore, the so-called azimuthal mode decomposition (AMD) technique that allows the reduction of the computational burden for the data extraction is presented in Section 3.3. The cubical scanning for near-field antenna measurement is also discussed in Section 3.3. Finally, summery of the contributions of this thesis is presented in Section 3.4.

3.1 Double directional channels

According to the double directional channel concept, the radio channel is divided into the propagation channel and antennas. The propagation channel considers multipath components as discrete plane waves departing from the transmitting antenna and arriving at the receiving antenna through the propagation environment. The multipath components are defined with specific parameters, e.g., complex amplitudes, AoAs, AoDs, delays, and polarizations. Considering a MIMO link as illustrated in Figure 3.1, the input-output relation is given by

$$\bar{y}_r = \bar{\bar{H}}\bar{x} + \bar{\xi}, \tag{3.1}$$

where $\bar{\bar{H}} \in \mathbb{C}^{N_r \times N_t}$ is the radio propagation channel transfer matrix mapping the transmit signals $\bar{x} \in \mathbb{C}^{N_t \times 1}$ to the receive signals $\bar{y}_r \in \mathbb{C}^{N_r \times 1}$; $\bar{\xi} \in \mathbb{C}^{N_r \times 1}$ represents the complex white Gaussian noise at the receiving antenna ports.

It has been known for a long time that the multipath components seem to arrive in concentrated bundles which are referred to as clusters and are understood as propagation paths diffused in space, either or both in delay and angle domains. Generally, angular power spectrum (APS) of the clusters is modeled by, e.g., Laplacian–distribution that is defined by nominal AoA/AoD and angular spread of arrival and departure (ASA/ASD). In multipath channels, the statistical distributions of the APS corresponding to the horizontal and vertical polarization are decoupled in azimuth and elevation directions, and such channels are referred to as three dimensional (3D) channel. The power azimuth spectrum (PAS) and power elevation spectrum (PES) in 3D models are defined separately. In two dimensional (2D) channel models such as SCM, SCME, WINNER II and IMT-Advanced, the APS is limited to the horizontal plane with Laplacian-distributed PAS [27-33].

An (u,s)−th entry of the MIMO channel matrix in (3.1) represents a radio channel from s −th transmitting antenna element to u −th receiving antenna element, which can be written in a 2D case as [27]

$$H_{u,s}(t,\tau) = \sum_{k_0=1}^{K}\sum_{l=1}^{L_{k_0}} e^{id_s k\sin(\phi_{k_0,l})}\begin{bmatrix}F_{\mathrm{tx,s,V}}(\phi_{k_0,l})\\ F_{\mathrm{tx,s,H}}(\phi_{k_0,l})\end{bmatrix}^{\mathrm{T}}\begin{bmatrix}\alpha_{k_0,l,\mathrm{VV}} & \alpha_{k_0,l,\mathrm{HV}}\\ \alpha_{k_0,l,\mathrm{VH}} & \alpha_{k_0,l,\mathrm{HH}}\end{bmatrix}$$

$$\begin{bmatrix}F_{\mathrm{rx,u,V}}(\psi_{k_0,l})\\ F_{\mathrm{rx,u,H}}(\psi_{k_0,l})\end{bmatrix} e^{id_u k\sin(\psi_{k_0,l})}e^{i2\pi\nu_{k_0,l}t}\delta_0(\tau-\tau_{k_0,l}). \quad (3.2)$$

The k_0 is the number of clusters, $1 \le k_0 \le K$; and l is the multipath index inside a cluster, $1 \le l \le L_{k_0}$; ϕ and ψ are the azimuth angle of departure and arrival; d_s and d_u are the distances of the $s-$th transmitting and $u-$th receiving antenna elements from the phase center of the each antenna array; F_{tx} and F_{rx} are the radiation patterns of the transmitting and receiving antennas measured at the coordinate origin, respectively. The subscripts V and H represent the vertical and horizontal polarizations, respectively; $\alpha_{k_0,l}$ are the polarimetric path gain; and $\nu_{k_0,l}$ is the Doppler shift of path k_0, l. The δ_0 is the Dirac delta function. α's, ψ's, and ϕ's define the APS of the propagation channel. Considering all the entries the size of the channel matrix of the MIMO link at a discredited time instant t becomes $\bar{\bar{H}}_t \in \mathbb{C}^{N_r \mathrm{x} N_t}$ where $1 \le t \le T$.

3.2 Multimode representation of channels

The multimode representation of the channel and antenna by means of SWE of the electromagnetic field has been discussed in [5]. The receive signals, $\bar{y}_r$ in (3.1) can be approximated by means of a radiated far-field from the transmit antenna array as [5, 36-37]

$$\bar{y}_r = \bar{\bar{R}}\bar{a} + \bar{\xi}, \quad (3.3)$$

where, $\bar{\bar{R}} \in \mathbb{C}^{N_r \times J}$ is the antenna receiving coefficients, characterizes the receive N_r –port antenna described by J spherical wave modes, and $\bar{a} \in \mathbb{C}^{J\times 1}$ is a vector containing the expansion coefficients of incoming waves. $\bar{\bar{R}}$ is known from measurements or from analytical models, whereas $\bar{a}$ can be obtained from computer simulations or extracted from channel sounding measurements. It is noted that (3.3) gives the information at one side of the channel, more specially, the receive side. However, for MIMO links, it is required to characterize the channel at the transmit side too. The transmitted

signals, $\bar{x}$, are mapped into the outgoing SWE coefficients of, $\bar{Q} \in \mathbb{C}^{J\times 1}$, by the antenna transmitting coefficients $\bar{\bar{T}} \in \mathbb{C}^{J\times N_t}$, as

$$\bar{Q} = \bar{\bar{T}}\,\bar{x}\,. \tag{3.4}$$

The channel is then described as the $\bar{\bar{M}} \in \mathbb{C}^{N_r\times N_t}$ matrix [5], which maps the modes excited by the transmitting antenna to the modes exciting the receive antennas or the vice versa as shown in Figure 3.2. The mapping between the outgoing waves $\bar{Q}$ at the Tx and the incoming waves $\bar{a}$ at the Rx can then be written as

$$\bar{a} = \bar{\bar{M}}\bar{Q}. \tag{3.5}$$

Hence, combining (3.3) – (3.5), the input-output relation for a MIMO link is defined as [5]

$$\bar{y}_r = \bar{\bar{R}}\bar{\bar{M}}\bar{\bar{T}}\bar{x} + \bar{\xi}, \tag{3.6}$$

where the MIMO channel matrix $\bar{\bar{H}}$ is expressed as

$$\bar{\bar{H}} = \bar{\bar{R}}\bar{\bar{M}}\bar{\bar{T}}. \tag{3.7}$$

One of the important issues in the propagation modeling is antenna de-embedding. Such propagation channel responses, $\bar{\bar{M}}$ allows complete antenna de-embedding, and hence, once such a channel matrix is available, it can then be applied, e.g., for MIMO and ultra wide band performance studies of arbitrary antennas both at the Tx and Rx without a need to repeat the measurement every time for a new transmit or receive antenna [38-40, **IV**].

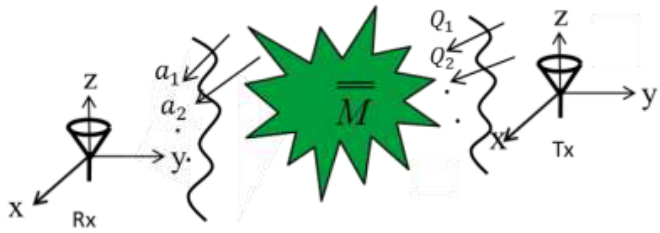

Figure 3.2. Representation of the propagation channel with antennas.

3.3 Method

In the spherical wave modeling, one needs not only to perform the measurements and modeling but also to develop proper measurement methodologies, which provide the possibility for appropriate data extraction. From the theoretical point of view, spherical scanning would be evidently the

optimum way to perform the scanning for the purposes of spherical wave characterization of the propagation channels. It is known from the spherical wave theory that in the case of a spherical scan surface, the required excitations for generating any spherical wave mode are very well-known and the spherical wave generation is robust and stable [21]. Although being obviously the optimum in theory, the spherical scanning for the channel measurement purposes may be impractical in some situations compared to, e.g., linear scanning. Linear scanners are very widely used in laboratories, and they clearly provide a possibility for both practical and fast scanning of large volumes. The disadvantage of the linear scanning is, however, that it does not readily support spherical wave characterization of the radiation channels, i.e., finding out the response of the channel against different spherical mode excitations of an antenna. Essentially, linear scanning supports well the acquisition of cubical scan data. This thesis analyzes the relations between the cubical scanning and spherical wave characterization of the radio channels, and methods of calculating the required spherical mode responses of the channel from the data acquired using cubical scanning. The practical and fast ways of robust data extraction of the parameters of general near- and far-field radio channels are examined with the possibility to include the effect of general antenna patterns [**I**–**II**], [**IV**]. Hence, application of such a scanning technique both at the Tx and Rx allows the generation of complete spherical-mode to spherical-mode channel matrix by measurements.

Spherical near-field antenna measurement is a well-established technique for determining the 3D radiation pattern of an antenna, where SWE is used to model the antenna radiation. It is a natural choice for many applications because if offers both a practical measurement geometry and a possibility for a conventional mathematical formulation of the problem. It is seen from (2.6), that the radiated field is completely determined by the antenna coefficients of the SWE. The purpose of the spherical antenna measurement is to find the unknown antenna coefficients by performing the scanning on a spherical surface. The fact that linear scanners also provide a convenient option for gathering measurement data on a cubical surface makes the cubical surface scanning an interesting possibility for 3D pattern measurement. In this thesis, cubical surface scanning is also applied for near-field antenna measurement and for related NF-FF transformations [**III**].

3.3.1 Cubical scanning geometry

This section presents the cubical surface geometry and scanning scheme used for generating the mode field in the application of spherical-wave modeling and near-field antenna measurements [**I**−**IV**]. A virtual cube is considered centered in the Cartesian coordinate system (x, y, z) such that there are $N_1 \times N_1$ sampling locations on each face of the cube. Each face of the cube is divided into $N_1 \times N_1$ smaller squares of equal size, and the sampling locations are at the centers of these squares leading to $N_C = 6 \times N_1^2$ sampling locations in total. There is some difference in the scanning scheme for the mode field synthesis and near-field antenna measurement applications. For field synthesis, scanning is performed for three orthogonal probe polarizations at each sampling location [**I**−**II, IV**] whereas for the NF-FF transformation in near-field antenna measurements, scanning is performed for two tangential polarizations [**III**].

In [41], the cubical scanning is examined for two different cases: i) scanning with only two tangential electric Hertzian dipoles and ii) scanning with two tangential electric and two tangential magnetic Hertzian dipoles. It is found out that the cubical scanning with two tangential electric dipole probes does not give a possibility to generate all the desired spherical wave modes accurately. On the other hand, including both the electric and magnetic dipole probes provided the possibility to generate all the desired spherical wave modes accurately. This is in line with the Huygens' Principle. However, in a practical measurement scenario this would evidently and unfortunately mean that one should use two different types of probes. Hence, the three orthogonal probes polarization is used for generating any arbitrary fields. An example for $N_1 = 4$ with the length of the side of the cube a is shown in Figure 3.3.

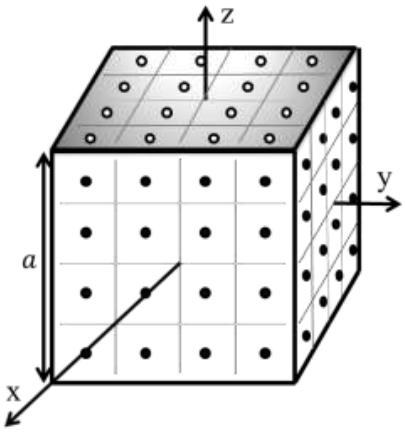

Figure 3.3. Cube Scanning Geometry for $N_1 = 4$.

3.3.2 Field synthesis using direct matrix method

This section deals with the synthesis of the radiated field using the cubical scanning technique either at the Tx or Rx side shown as in Figure 3.2. The radiated electric far field of any desired spherical wave mode j, and only this mode is referred to as target field and presented by vector $\bar{\bar{E}}_{tar,j}$ [**I**]. $\bar{\bar{E}}_{tar,j}$ is calculated using (2.6) with $c = 3$. Then the target is to find out a set of complex input signals $\bar{x}_j$ for the probe in the different sampling locations and polarizations such that the sum field radiated by the probe in the different sampling locations and polarizations would equal to the target field. The approach to find out the input signals is to match the probe fields to the target field [**I**]. In a matrix form, the relation between $\bar{\bar{E}}_{tar,j}$ and $\bar{x}_j$ is as follows [**I**]

$$\bar{\bar{E}}_C \bar{x}_j = \bar{\bar{E}}_{tar,j}, \tag{3.8}$$

where

$$\bar{\bar{E}}_{tar,j} = \bar{\bar{F}} \bar{Q}_j \,. \tag{3.9}$$

$\bar{\bar{F}} \in \mathbb{C}^{2L \times J}$ contains the spherical far-field pattern function of each single spherical wave mode which is independent of radial component and L is the number of angular samples of the antenna far-field pattern. The vector $\bar{Q}_j$ contains '1' in an j −th of $\bar{Q}_j$ and '0' in all other entries. The coupling matrix $\bar{\bar{E}}_C \in \mathbb{C}^{2L \times N_T}$ consists of complex electric fields of all antenna elements of the virtual array. The number of unknowns $N_T = 3N_C$, is the number of sampling locations on the cube times the number of probe polarizations. Then the input signals to the virtual array for exciting the j −th spherical wave mode $\bar{x}_j$ is calculated using (3.8) through a matrix inversion as

$$\bar{x}_j = \bar{\bar{E}}_C^{\dagger} \bar{\bar{F}} \bar{Q}_j \,, \tag{3.10}$$

where † denotes the pseudo inverse. Finally, these signals are applied on the probes over the cubical surface for the generation of the synthesized target field vectors $\bar{\bar{E}}_{syn,j}$ for all spherical wave modes.

In practical measurements or scanning scenarios, the measured data is always contaminated by noise. It is also well-known that inverses may amplify noise. Hence, the stability of the pseudo inverse in (3.10) may be a problem when there is too much noise. Therefore, the noise sensitivity of the cubical scanning is analyzed by introducing certain noise level in the input signals of the probes. A complex white Gaussian noise resembling the measurement uncertainty is added to the input signals, i.e., $\bar{x}_{j,no} = \bar{x}_j + \rho \bar{\mathrm{N}} \times \bar{x}_j$, where entries of $\bar{\mathrm{N}}$ are given by $\mathcal{CN}(0,1)$. Here $\bar{x}_{j,no}$ consists of the noisy signals,

$\rho = 10^{-2}$ is used as noise amplitude. The synthesized field, $\bar{E}_{syn\_no,j}$ for each spherical wave mode is then calculated using the following equation

$$\bar{E}_{syn\_no,j} = \bar{\bar{E}}_C \bar{x}_{j,no}. \tag{3.11}$$

The robustness of spherical wave mode generation over a 2-octave band for different cubical scan schemes of $N_1 = 5 \dots 10$ for $a/\lambda = 0.6 \dots 2.4$ is investigated [42]. In order to evaluate the accuracy of the spherical mode generation, maximum normalized n-mode error $\varepsilon_n(n)$ [**I**] is analyzed in the presence of noise. The $\varepsilon_n(n)$ reflects the maximum error in generating spherical wave modes as a function of n, and it likewise leads to an insight on how many sampling locations per cube side, are required to generate any spherical wave mode up to $n = N$ within the maximum allowable error level. The $\varepsilon_n(n)$ is defined as

$$\varepsilon_n(n) = \max\left[\epsilon_t\left((2(n-1)(n+1)+1\right) \dots 2n(n+2))\right], \tag{3.12}$$

where $\epsilon_t\ (j) = \max\left[\frac{|\bar{E}_{syn\_no,j} - \bar{E}_{tar,j}|}{\max|\bar{E}_{tar,j}|}\right]$ is the maximum error between the target $\bar{E}_{tar,j}$ and the synthesized $\bar{E}_{syn\_no,j}$ field vector as a function of spherical wave mode j [**I**].

The significant factors, which influence the uncertainty in generating the spherical wave modes up to a certain spherical mode index, are the cube size in wavelengths and the number of samples. The natural explanation for this is the cut-off property of the spherical wave series. When the cube size in wavelengths increases, this cut-off occurs at a higher truncation number N. Also increasing N_1 generally lowers the uncertainty.

It is anticipated that the post processing of the measured data required by the cubical surface scanning is computationally intense [**I**, **IV**, 38, 42]. Hence, any technique to reduce the computational burden would be beneficial. In the next subsection, the AMD technique is presented in the application of the spherical mode field synthesis, which provides the possibility to reduce the computational burden of the matrix inversion in (3.10).

3.3.3 Field synthesis using azimuthal mode decomposition method

The AMD technique is presented in [**II**] to be applied in connection with cubical surface scanning and subsequent data processing. The AMD technique can be applied as a preprocessing step to reduce the computational burden of the data processing. The method is applicable with a general probe as it is independent of the probe pattern.

Field synthesis using the direct matrix method does not pose any strict requirements either for the sampling locations or for the probe orientations and polarizations as far as (3.8) remains well conditioned. In other words, the sampling locations do not need to be equally spaced on each surface as shown in Figure 3.3. However, the use of AMD does have certain specific requirements. These requirements are related firstly to scanning locations and secondly to probe orientations and polarizations in sampling locations. These two requirements are discussed in the following subsections.

Requirement for scanning locations

As a starting point, let us consider a cubical surface scanning geometry as illustrated in Figure 3.3 with the example case with $N_1 = 4$. It is easily noticeable that the cube surfaces can be divided into $N_1 + 2$ layers with different z coordinates as shown in Figure 3.4(a). The z coordinates of the layers 1 to 6 in this example are $0.5a$, $0.375a$, $0.125a$, $-0.125a$, $-0.375a$, and $-0.5a$, respectively. The sampling locations at layers 1 and 6 are shown in Figure 3.4(b), and those for the layers 2 to 5 in Figure 3.4(c).

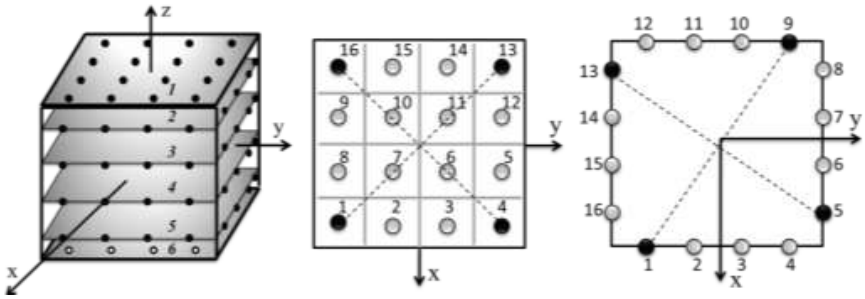

(a) (b) (c)

Figure 3.4. (a) Scanning locations on $N_1 + 2 = 6$ (numbered from 1 to 6) layers along the z axis. (b) Probe locations for layers 1 and 6. (c) Probe locations for 2 to 5.

The requirement for scanning locations is that one must be able to divide all the sampling locations to subsets of four sampling locations in such a way that the four sampling locations in each subset are separated by 90^0 in φ but their θ and r coordinates are the same. This leads to the fact that the sampling locations 1, 5, 9, and 13 in Figure 3.4 (c) form one subset fulfilling the scanning requirement. Similarly, the sampling locations 2, 6, 10, and 14 form one subset fulfilling the scanning requirement and it is clear that ultimately all the sampling locations can be divided into subsets of four sampling locations on layers 2 to 5. It is also clear that the sampling locations can be divided equally well into subsets of four sampling locations also on layers 1 and 6.

Requirement for probe orientations and polarizations

The second requirement concerns the probe orientations and polarizations. As said earlier, generally three orthogonal probe polarizations are needed at each sampling location for the field synthesis. The requirement for the probe orientations and polarizations is that they remain the same in terms of the spherical $r, \theta,$ and φ unit vectors in all those sampling locations that belong to one subset of four sampling locations. This is equal to what one would have if the traditional φ scanning with 90^0 increment in φ irrespective of the probe is performed.

Let us consider one subset of four sampling locations, e.g., the locations 1, 5, 9, and 13 on layer 2 (see Figure 3.4(c)), and let us assume that the probe in the sampling location 1 is $x-$ oriented and $y-$ polarized. Then the probe orientations and polarizations in the probe locations 5, 9, and 13 must be y and $-x$, $-x$ and $-y$, and $-y$ and x, respectively. For clarity, this example case is illustrated in Figure 3.5, where the dashed long arrows represent the probe orientation vectors and solid short arrows represent the probe polarization vectors.

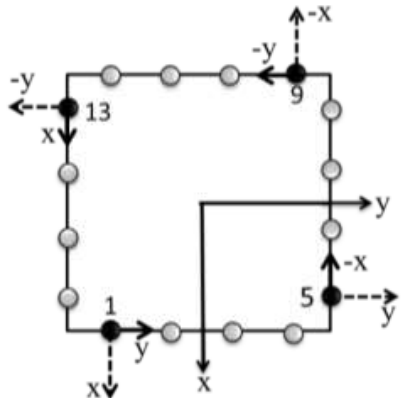

Figure 3.5. The probe orientations (dashed long line) and polarizations (solid short line) with 90^0 separation in φ.

Principle of AMD

It is noted that (2.6) can be rewritten by using the azimuthal m-mode truncation as [21]

$$\bar{E}(r,\theta,\varphi) = \sum_{m=-M}^{M} \bar{C}_m(r,\theta)\, e^{im\varphi} \tag{3.13}$$

with

$$\bar{C}_m(r,\theta) = k\sqrt{\eta_0}\sum_{s=1}^{2}\sum_{n=\max(1,|m|)}^{N} Q_{smn}\frac{\bar{F}_{smn}^{(3)}(r,\theta,\varphi)}{e^{im\varphi}}, \tag{3.14}$$

where $\bar{C}_m(r,\theta)$ is the azimuthal mode coefficients of the field. The scanning requirements for probe locations and for the probe orientations and polarizations discussed in the previous two subsections imply that the term $\bar{C}_m(r,\theta)$ in (3.13) remains the same for the field radiated by the probe for all the sampling locations in each subset of four sampling locations since the θ and r coordinates are the same for these four sampling locations. The key principle of the AMD is the exploitation of the following orthogonalities with (3.13):

$$\frac{1}{4}\sum_{p=1}^{4} e^{im(\varphi+\varphi_p)} = [\dots \delta_{-4m} + \delta_{0m} + \delta_{4m} \dots]e^{im\varphi}, \qquad (3.15a)$$

$$\frac{1}{4}\sum_{p=1}^{4} e^{-i\varphi_t} e^{im(\varphi+\varphi_p)} = [\dots \delta_{-3m} + \delta_{1m} + \delta_{5m} \dots]e^{im\varphi}, \qquad (3.15b)$$

$$\frac{1}{4}\sum_{p=1}^{4} e^{-i2\varphi_t} e^{im(\varphi+\varphi_p)} = [\dots \delta_{-2m} + \delta_{2m} + \delta_{6m} \dots]e^{im\varphi}, \qquad (3.15c)$$

$$\frac{1}{4}\sum_{p=1}^{4} e^{-i3\varphi_t} e^{im(\varphi+\varphi_p)} = [\dots \delta_{-1m} + \delta_{3m} + \delta_{7m} \dots]e^{im\varphi}, \qquad (3.15d)$$

where $[\varphi_1, \varphi_2, \varphi_3, \varphi_4] = [0, \pi/2, \pi, 3\pi/2]$, and $\delta_{m'm} = 1$ for $m = m'$ while $\delta_{m'm} = 0$ for $m \neq m'$(Kronecker delta). By applying these orthogonalities one can form the following equations for each subset as

$$\bar{E}_0(r,\theta,\varphi) = \frac{1}{4}[(+1)\bar{E}(r,\theta,\varphi) + (+1)\bar{E}(r,\theta,\varphi+\pi/2) + (+1)\bar{E}(r,\theta,\varphi+\pi) + (+1)\bar{E}(r,\theta,\varphi+3\pi/2)] \qquad (3.16a)$$

$$\bar{E}_1(r,\theta,\varphi) = \frac{1}{4}[(+1)\bar{E}(r,\theta,\varphi) + (-j)\bar{E}(r,\theta,\varphi+\pi/2) + (-1)\bar{E}(r,\theta,\varphi+\pi) + (+j)\bar{E}(r,\theta,\varphi+3\pi/2)] \qquad (3.16b)$$

$$\bar{E}_2(r,\theta,\varphi) = \frac{1}{4}[(+1)\bar{E}(r,\theta,\varphi) + (-1)\bar{E}(r,\theta,\varphi+\pi/2) + (+1)\bar{E}(r,\theta,\varphi+\pi) + (-1)\bar{E}(r,\theta,\varphi+3\pi/2)] \qquad (3.16c)$$

$$\bar{E}_3(r,\theta,\varphi) = \frac{1}{4}[(+1)\bar{E}(r,\theta,\varphi) + (+j)\bar{E}(r,\theta,\varphi+\pi/2) + (-1)\bar{E}(r,\theta,\varphi+\pi) + (-j)\bar{E}(r,\theta,\varphi+3\pi/2)] \qquad (3.16d)$$

where $\bar{E}_0, \bar{E}_1, \bar{E}_2$, and $\bar{E}_3$ are the weighted sum patterns of each subset of four sampling locations. Due to the orthogonalities in (3.15) the SWEs of the sum fields $\bar{E}_0, \bar{E}_1, \bar{E}_2$, and $\bar{E}_3$ can be written as

$$\bar{E}_0 = \sum_{m=-M\dots-4,0,4,\dots M} \bar{C}_m(r,\theta)\, e^{im(\varphi+\varphi_p)} \qquad (3.17a)$$

$$\bar{E}_1 = \sum_{m=-M\ldots-3,1,5,\ldots M} \bar{C}_m(r,\theta)\, e^{im(\varphi+\varphi_p)} \tag{3.17b}$$

$$\bar{E}_2 = \sum_{m=-M\ldots-2,2,6\ldots M} \bar{C}_m(r,\theta)\, e^{im(\varphi+\varphi_p)} \tag{3.17c}$$

$$\bar{E}_3 = \sum_{m=-M\ldots-1,3,7,\ldots M} \bar{C}_m(r,\theta)\, e^{im(\varphi+\varphi_p)}. \tag{3.17d}$$

In these equations, it becomes literally expressed that three out of four azimuthal modes disappear. As a result the number of unknowns in each expansion is smaller, as compared to (3.13), by a factor of four. Now instead of applying the direct matrix method on (3.13) it is applied on (3.17). In this way, instead of having one system of linear equation like (3.8), four system of linear equations are obtained that can be written as

$$\bar{\bar{E}}_0 \bar{x}_j^0 = \bar{E}_{tar,j}^0 \tag{3.18a}$$

$$\bar{\bar{E}}_1 \bar{x}_j^1 = \bar{E}_{tar,j}^1 \tag{3.18b}$$

$$\bar{\bar{E}}_2 \bar{x}_j^2 = \bar{E}_{tar,j}^2 \tag{3.18c}$$

$$\bar{\bar{E}}_3 \bar{x}_j^3 = \bar{E}_{tar,j}^3 \tag{3.18d}$$

The set of input signals $\bar{x}_j$ can be found by solving (3.18). For example, for synthesizing the mode field with $m = 0$, the (3.18a) needs to be solved and the number of unknown to be found here is four times less that in (3.8), and the same goes for synthesizing the other modes as well. It is important to mention that one must solve the right equation depending on the mode that needs to be synthesized. With the reduced number of unknowns, the dimensions of the coupling matrices $\bar{\bar{E}}_0, \bar{\bar{E}}_1, \bar{\bar{E}}_2$, and $\bar{\bar{E}}_3$ in (3.18) are reduced by the factor of four as compared to that in (3.8). The computational burden of inverting (3.18) is reduced by a factor that is depended on the computer complexity of the matrix inversions.

3.3.4 Near-field to far-field transformation

Cubical surface scanning is a fascinating idea because it can be realized using linear scanning on six faces of a cube and hence, it provides the possibility to determine the complete 3D pattern instead of the pattern in a limited angular region as in traditional linear scanning. In [**III**], an investigation on the applicability of the cubical surface scanning for extracting the antenna coefficients from the SWE for determining the far-field radiation pattern is

presented. The analytical and discrete solution for the antenna coefficients are extensively discussed in [23]. In this thesis only discrete, in particularly, matrix inversion technique is used.

The starting point of this work is the modeling of the antenna pattern using SWE. The ultimate goal is then to find computationally efficient and robust methods for the extraction of the antenna coefficients from the cubical scan data. It is noted that a straightforward method for finding the coefficients would be the direct matching of spherical wave modes to the measured samples on a cubical surface through the matrix inversion technique [23]. Instead of the direct matching, a two-step technique for finding the coefficients is presented in [**III**]. The AMD technique discussed in Section 3.3.3 is performed in the first step to reduce the computational burden of the direct matrix inversion. Although the second step remains computationally inefficient, it is anticipated that the computational complexity in the second step can be reduced by the application of some sophisticated techniques [43].

In [**III**], the same scanning scheme described in Section 3.3.1 is considered for the application to the near-field antenna measurement with the exception of having the scanning for two tangential polarizations, instead of three polarizations. Computer calculations for simulating the cubical near-field antenna measurements are carried out for the certain antenna model with the electric Hertzian dipole probe for several different cases by varying the cube sizes and the sampling distance. The noise sensitivity of the related NF-FF transformations is analyzed for both direct matrix inversion technique and the matrix inversion technique with the AMD. The results show the feasibility of cubical surface scanning for extracting the coefficients up to a certain truncation number accurately and more importantly, show the feasibility of the AMD for this application that allows a reduction in the computational burden of the NF-FF transformation.

3.4 Summary of the contributions of this thesis

In spherical wave modeling, the channel is treated as a spherical-mode to spherical-mode channel matrix, which relates each outward propagating spherical mode at the Tx to that of the inward-propagating spherical mode at the Rx. In [**I**], the generation of a spherical-mode to spherical-mode channel matrix from data measured on a cubical scan surface, is investigated. It is shown that scanning with three orthogonal probe polarizations on a cubical scan surface, and by using the virtual array principle, provides a possibility

for generating each spherical mode independently. Nonetheless, the post-processing of the measured data required by the cubical surface scanning is computationally intense. The AMD technique for the reduction of the computational burden for generating the spherical-mode to spherical-mode channel matrix is presented in [**II**].

The cubical scanning technique is further investigated for the near-field antenna measurement and related NF-FF transformations in [**III**]. The AMD technique is also applied for a reduction in the computational burden of the NF-FF transformations. The results show not only the applicability of the cubical surface scanning for the transformation but also feasibility of the AMD technique in this context.

4. Spatial degrees of freedom in propagation channels

It is of general interest among antenna research community how to improve the multi-element antenna design for multi-antenna technology, e.g., MIMO under a certain size limitation to have the spatial diversity and multiplexing efficiently. In contrast, the propagation research community concerns on channel modeling in order to test the designed multi-antenna systems in real propagation scenario. In Chapter 3, the channel modeling based on SWE introduced and the method for estimating the propagation channel responses in this context is proposed. In [**IV**], the proposed method is applied in estimating the DoF of the spatial propagation channel. It is obvious that implementing more antenna elements than the DoF of the spatial propagation channel leads to redundancy.

The DoF is a measure of the effective number of the antenna elements that can meaningfully exploit the multipath richness of the channel for spatial multiplexing or diversity. It depends on multipath richness of the propagation channel and antenna aperture size only, and provides an upper bound on the number of eigenchannels that any element geometry on the antenna aperture can realize under the given propagation conditions. In this thesis, the DoF of the multipath channels is derived by means of the SWE of the electromagnetic fields radiated from the antenna array having a certain aperture size. An estimation of spatial DoF from measured multipath propagation channels in the multiple-input single-output (MISO) regime is presented [**IV**]. The DoF of the multipath channels on the transmit antenna having a certain aperture in the propagation channel is derived. An antenna array presented in Section 3.3.1 is considered at the transmit side. The presented DoF estimation method is easily extendable to the MIMO scenarios in a straightforward manner, which is reported in [39-40].

In this chapter, the spatial DoF of the propagation channels based on the SWE of the electromagnetic field is discussed. Section 4.1 gives a formulation of the MISO channel in a space and a spherical wave domain, where their interrelationship is described. Section 4.2 discusses the DoF of multipath channels in an indoor environment. Finally, the summary of the contributions of this thesis is given in Section 4.3.

4.1 Spatial DoF of the MISO propagation channels

This section initially shows an approximation of the MISO channel using the SWE and discusses the relationship with the conventional MISO channel described in space. Finally, the DoF of the MISO propagation channel expressed by the spherical wave coefficients is shown which provides an upper bound of the spatial DoF for a transmit antenna having a certain aperture in the propagation channel.

4.1.1 SWE of MISO channel

An expression of the MISO propagation channel using the SWE is formulated. Likewise, MIMO channel (3.1), MISO narrowband system in an equivalent baseband form is defined as

$$y_r = \bar{H}\bar{x} + \xi. \tag{4.1}$$

In MISO link, the number of antenna element at the Rx is $N_r = 1$, hence in (4.1), y_r becomes a scalar and $\bar{x}$, $\bar{H} \in \mathbb{C}^{N_t \times 1}$ are the vectors. Moreover, the representation of the received signal in spherical wave domain becomes [5, 36-37]

$$y_r = \bar{r}\bar{Q} + \xi, \tag{4.2}$$

where $\bar{Q} \in \mathbb{C}^{J \times 1}$ is the vector of the spherical-wave modes on the transmit side, and $\bar{r} \in \mathbb{C}^{1 \times J}$ is the mode coupling vector from transmit far field to the output of the receive antenna port. It should be noted that the receive antenna effects are included in $\bar{r}$. The vector $\bar{r}$ is defined as the propagation channel response in the MISO regime. The vector $\bar{Q}$ is related to the input to the transmit antenna array $\bar{x}$ as [21]

$$\bar{\bar{E}}_C\bar{x} = \bar{\bar{F}}\bar{Q} \tag{4.3}$$

The dimension of $\bar{\bar{F}}$ and $\bar{\bar{E}}_C$ are defined in (3.8-3.9). Using (4.2) and (4.3), (4.1) is translated into

$$y_r = \bar{r}\bar{\bar{F}}^{\dagger}\bar{\bar{E}}_C\bar{x} + \xi. \tag{4.4}$$

4.1.2 Spatial DoF in the MISO regime

The DoF in the MISO regime can be explained by the SWE in (4.4). The number of dominant spherical wave modes is determined by the transmit antenna aperture size because of the mode truncation property (2.5). As the truncation N in (2.5) is related to the total number of dominant spherical wave modes J, then larger antenna aperture can support more spherical wave modes to propagate over the channel, which leads to larger DoF. The DoF of the propagation channel D_{r} is given by the number of linearly independent coefficients in $\bar{r}$ as

$$D_{\mathrm{r}} = \mathrm{rank}(\bar{\bar{r}}_{\mathrm{r}}) \tag{4.5}$$

where $\bar{\bar{r}}_{\mathrm{r}} = E[\bar{r}^H \bar{r}]$ is the correlation matrix of the MISO propagation channel response, $E[\cdot]$ is the ensemble average to make $\bar{\bar{r}}_{\mathrm{r}}$ full rank, $(\cdot)^H$ denotes the conjugate transpose, and rank(·) computes a rank of the correlation matrix. It must be emphasized again that the DoF is affected by the receive antenna properties in this analysis of the MISO regime.

4.2 Measurement-based analysis of DoF

The cubical scanning method presented in Section 3.3.1−3.3.2 is applied to estimate the MISO propagation channel response $\bar{r}$ from practical radio sounding. It involves design of the transmit signal and antenna array configuration. The transmit signals from the antenna array for exciting the j −th spherical wave mode $\bar{x}_j$ is calculated using (3.10) and the propagation channel response of the j −th spherical wave mode r_j becomes from (4.1) and (4.2) as

$$r_j = \bar{\bar{H}}\bar{x}_j. \tag{4.6}$$

This way the required J −independed samples of $\bar{r}$ is obtained. The rank of the correlation matrix (4.5) is estimated by its eigenvalues. In [**IV**], the methodology for designing the transmit signal and transmit antenna array is verified with the radio channel measurements performed in the anechoic chamber and the result provides a sound estimation for DoF. The method is then applied to estimate the DoF in indoor MISO multipath channels with varying environmental conditions. The results show that the DoF on the transmit side of the considered channels are higher when the antenna aperture size is increased at a fixed frequency, and when the frequency increases for a fixed antenna aperture size. Furthermore, for a fixed frequency, increasing the antenna aperture size is more effective in observing

extra DoFs in obstructed and non-line-of-sight (NLOS) channels than in the line-of-sight (LOS) channels. It is also shown that for a fixed antenna aperture size, the use of the higher frequency brings larger DoFs in many propagation scenarios. Finally, the solid angle of multipath, metric of multipath richness defined as an angular range of dominant multipath subtended on a unit sphere is derived.

4.3 Summary of the contribution of this thesis

The spatial multiplexing is one of the most promising techniques for increasing the channel capacity by exploiting eigenmodes of radio channels for parallel data streaming. The potential of the spatial multiplexing in radio channels is discussed by several metrics, such as the channel capacity, the number of dominant eigenmodes, and the eigenvalue dispersion [44], and the evaluation of these metrics are restricted by the certain antenna configurations. In order to obtain more generic estimates of the metrics for various antenna types, the DoF of the spatial propagation channel is evaluated in this thesis. The DoF depends on the radio propagation condition and the antenna aperture size, but is otherwise independent of the antenna elements and geometry, and indicates the effective number of antenna elements on the aperture that can contribute to the increase of the channel capacity through spatial multiplexing.

The work in [**IV**] provides an experimental method for estimating the spatial DoF of a wireless propagation channel. The work is based on SWE of the electromagnetic field. The method serves as an experimental validation and proof of previous theoretical work on the topic, i.e., the expansion of electromagnetic fields in spherical wave modes for an antenna independent representation of the wireless channel [5, 36-37, 45-46] and general antenna-channel interaction analysis [5] and DoF of multiple antenna channels [47-48]. In addition, the work in [**IV**] strives to shed light on a number of related questions, such as, the effect of increasing the frequency when the antenna aperture size is limited, or metrics for multipath richness.

5. Over-the-air test method for multi-antenna terminals

With the aim of evaluating overall communication performance that combines the performances of the mobile terminal antenna and the RF transceiver section in the device, OTA testing has become more popular in recent years. The existing standard of the OTA performance testing is meant for 2G and 3G mobile terminals with single antenna that is known as single-input single-output (SISO) OTA testing [14-15].

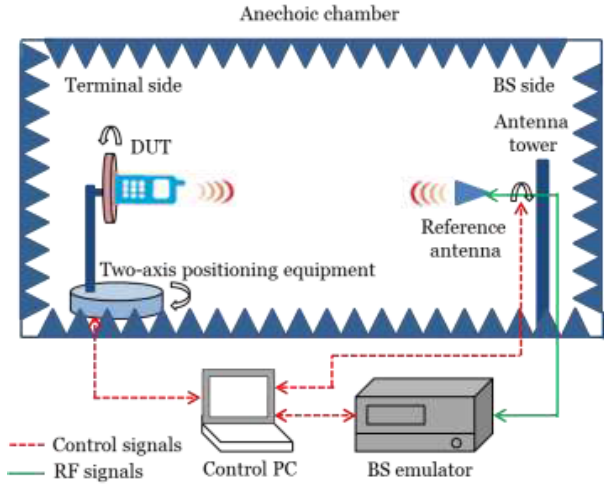

Figure 5.1. An illustration of the SISO OTA test facility in an anechoic chamber.

Total radiated power (TRP) for transmit performance and total radiated sensitivity (TRS) for receive performance were selected as the figure of merits (FoMs) for such OTA testing. These methods rely on a simple 3D radiation pattern measurement of the antenna by using the terminal's own RF transceiver section as an internal signal source, and by establishing a radio link with a base station (BS) emulator. The BS emulator emits the signal of

the suitable connection protocols for 2G and 3G technologies, e.g., GSM, CDMA, and TDMA. An illustration of the SISO OTA testing in an anechoic chamber is shown in Figure 5.1.

In Figure 5.1, the radio link is established between the device under test (DUT) and the BS emulator via a reference antenna installed on an antenna tower. Usually, dual−polarized reference antenna is used to measure both the vertical and horizontal components of the radiated field by the DUT. In addition, a 2D positioner is used to rotate the DUT in vertical and horizontal axes.

The MIMO technique is a key technology for evolving wireless technologies for 4G to enhance the capacity and throughput in multipath propagation environments. It is already known that the overall benefit of the MIMO technique is dependent not only on the characteristics of the multiple antennas but also on the spatial features of the propagation channel. Mobile terminals that include MIMO antenna pose new challenges and requirements for the OTA performance testing [49]. The most realistic way to evaluate the MIMO devices is to test them as they are exposed during their normal operation. For the accurate performance testing, the evaluation needs to be conducted using the BS, the multipath propagation channel, and real-world mobile terminal with multiple antennas. Standardization work for the development of the so-called MIMO OTA test methodologies is still ongoing and several approaches have been extensively discussed [50-52].

The remainder of this chapter is organized as follows. Section 5.1 briefly discusses the proposed performance parameters for MIMO OTA testing. Section 5.2 introduces the relevant channel models. In Section 5.3, an overview of different MIMO OTA test methodologies is presented. The channel emulation technique used in MIMO OTA testing is discussed in Section 5.4. Contributions of this thesis in this area are listed in Section 5.5.

5.1 Figure of merits

The FoMs TRP and TRS for SISO OTA performance testing do not take into account the propagation channel properties and are not sufficient for the correct characterization of the spatial behavior of a DUT with multiple antennas. Consequently, a clear need for the selection of the FoMs for the MIMO OTA testing has been raised. The FoMs must be such that it would able to distinguish a good device from a poor one. The FoMs currently considered in the standardization forum are listed in Table I.

As MIMO devices are defined to provide enhanced throughput, *MIMO throughput* becomes the predominant FoM for characterizing MIMO-capable user equipment (UE) performance. This active end-to-end throughput measurement attempts to emulate a realistic user experience by testing the data capacity under the influence of signal fading and in a usage environment [53, 55]. The *channel quality indicator* (*CQI*) defines the overall measurement of the channel conditions under a particular transmission mode [53]. The UE sends the *CQI* information to the BS so that BS can select appropriate modulation and coding scheme. The *TRP* is a measure of how much power the UE radiates and is defined as the integral of the power transmitted over the entire radiation sphere and *TRS* represents the lowest receiver sensitivity level of the UE's receiver. These metrics in categories 1 and 2 in Table 1 are called the active FoMs measured by establishing active communication link with the DUT with or without realistic fading effect on the measurement setup. For such measurement, the transmitted signal is typically delivered by a BS emulator.

Table 1. List of FoMs for MIMO OTA measurement [53.54].

Category	1	2	3	4
FoMs	MIMO throughput Channel quality indicator	TRP TRS	Gain imbalance Spatial correlation MIMO capacity	Antenna efficiency Mean effective gain

Characterization of the performance of MIMO antennas is also conducted using passive testing. The passive testing includes the characterization of the MIMO antenna radiation with respect to the FoMs of category 3 and 4 in Table 1. The antenna *gain imbalance* refers to the power imbalance between the antennas, including the long-term imbalance and the short-term imbalance. Long-term imbalance is introduced by the feeder line, RF channel, the antenna hardware and so on, and short-term imbalance is mainly caused by the shadow fading [56]. The *spatial correlation* measures the similarity of the received signals between different antenna elements under certain channel conditions [57]. The *MIMO capacity* can be estimated using the measured antenna patterns and the selected multipath channel model. It provides the theoretical maximum capacity achievable in a communication link with multiple antennas at both ends under a given propagation environment [58]. The antenna *efficiency* measures the losses at the antenna elements and the losses due to impedance mismatch. In general, the efficiency is defined as the ratio between the *TRP* and the accepted power at the

terminal [59]. The *mean effective gain* is an essential parameter that describes the statistical measure of the antenna gain in a realistic mobile environment [60-61]. These passive metrics can easily be evaluated using the measured antenna radiation pattern obtained from traditional chamber test methods.

5.2 Channel models

When developing simulation and test strategies for characterizing the performance of the MIMO UE under realistic channel conditions, it becomes important to develop channel models that accurately represent a spatially rich multipath environment. Several reference channel models have been proposed to characterize the MIMO channel in all the dimensions, i.e., frequency, time, space, and polarization. Thus the channels are double-directional and polarimetric in angular and temporal domains [62]. There are two basic types of channel models currently being studied for MIMO OTA testing: geometry-based models and correlation-based models. Examples for the geometry-based models are 3GPP Spatial Channel Model (SCM) [27], its extension (SCME) [28-31], WINNER II [32], IMT-Advanced [33] and COST2100 [34], and the Kronecker model [35] is in the family of the correlation-based models.

The geometric description of the propagation channel and the separation of the antenna and the propagation channel are essential requirements for the basic radio channel model to be reconstructed in a MIMO OTA test facility. Facilitating the double directional channel concept [26], i.e., the separation of propagation and antennas, the geometry-based channel models are realizable with a MIMO OTA test setup whereas the correlation-based channel models do not fulfil these prerequisites. In the correlation-based channel model, generic antenna characteristics are essential to the channel model, which means the model itself assumes specific DUT antennas. Hence, it becomes impractical to measure the real DUT performance to any further extent.

It is now noted that the MIMO channel matrix $\overline{\overline{H}}_t$ described in Section 3.1 is the quantity that is being reconstructed within the MIMO OTA test facility. Note that the right hand side of (3.2) can easily be separated into two terms: the impinging field including the transmitting antenna patterns and the pattern of the receiving antenna, also called DUT pattern in this thesis. When a single multipath component is incident from the $s-$th transmitting antenna, the impinging field observed at the $u-$th receiving antenna location is expressed as

$$\bar{E} = \begin{bmatrix} F_{\mathrm{tx,V}}(\phi) \\ F_{\mathrm{tx,H}}(\phi) \end{bmatrix}^{\mathrm{T}} \begin{bmatrix} \alpha_{\mathrm{VV}} & \alpha_{\mathrm{HV}} \\ \alpha_{\mathrm{VH}} & \alpha_{\mathrm{HH}} \end{bmatrix} e^{id_s k \sin(\phi)}\, e^{i2\pi\nu t}, \tag{5.1}$$

while the DUT pattern are then given by

$$\bar{G}_{DUT} = \begin{bmatrix} F_{\mathrm{rx,V}}(\psi) \\ F_{\mathrm{rx,H}}(\psi) \end{bmatrix} e^{ik \sin(\psi)}. \tag{5.2}$$

In (5.1), $\bar{E}$ describes the complex polarimetric amplitude of the time-harmonic impinging plane wave field. The MIMO OTA test facilities attempt to reproduce this field as accurately as possible for each single path and, as a more complex and realistic case, statistical distributions of the APS.

5.3 Summary of current MIMO OTA test methodologies

Several methodologies for MIMO OTA testing have been proposed for MIMO performance evaluation in the standardization forums [50-51] as well as in the scientific community [52]. These methodologies are strongly varied in terms of emulating propagation environment, complexity, and cost. Common to all these methods is that the test is performed either fully or partly OTA so that both the antenna and the propagation channel are taken into account with the purpose to be capable of creating an electromagnetic environment, which represents the true environment to which the device is exposed during its normal operation. The proposed MIMO OTA test methods can be categorized into three main approaches based on the channel emulation and test setup criteria:

- Channel emulator based multi-probe anechoic chamber method;
- Reverberation chamber method and
- Two-stage method.

Unless stated otherwise, a term “multi-probe method” is used to define the channel emulator based multi-probe anechoic chamber method in this thesis. In this method, a number of probes placed in different configuration around the DUT and a fading emulator is used to create a realistic and repeatable multipath environment in an anechoic chamber [63-75]. This method can reproduce any environment created by a reference channel model discussed in Section 5.2, as it does not pose any major theoretical limitation in emulating different channel conditions. In practice, however, this approach is somewhat costly due to space and required number of coherent output channels.

In the reverberation chamber method, the DUT and the transmitting antennas emulating the BS signal are placed inside of a reverberating chamber with conductive walls [76-79]. As the signal is fed through the transmitting antennas, the waves propagate inside the chamber reflecting seamlessly and randomly until they reach the DUT. Thus, the reverberation chamber is a cost effective way of reproducing a theoretical propagation channel where the AoAs of the waves are uniformly distributed over the angular domain. The difficulty with reverberation chamber methods is that they are not well-suited for emulating such channel conditions that would be in line with any geometry-based channel model, which has more directional selectivity.

The two-stage method is based on the knowledge that the antenna characteristics can be independently measured and then mathematically combined with the desired channel characteristics in the channel emulator. The first stage in the two-stage method involves the pattern measurement of the DUT over the air, and the second stage involves combining of the DUT patterns with the propagation channel data and running the MIMO performance test conductively [80-81]. Hence, the two-stage method poses requirements of special connectors to the antenna ports, which means that the test is never performed in the realistic usage conditions of the DUT such as the head effects.

5.4 Selected studies

Although multi-probe method is comparatively costly, from technical points of view it appears to be the most flexible one for MIMO performance evaluation. The focus of this thesis is on multi-probe method. Section 5.4.1 is devoted to describe the setup of the multi-probe method. Having defined the intended field (5.1), several emulation techniques are discussed to emulate such field. To the author's knowledge, the two most commonly used techniques are the prefaded signal synthesis (PFS) and plane-wave field synthesis (PWS). The PFS and PWS are discussed in Section 5.4.2 and some of their advantages and disadvantages briefly discussed in the following.

5.4.1 Setup of the multi-probe method

A schematic representation of the setup of a typical multi-probe method for MIMO OTA testing facility is illustrated in Figure 5.2, which consists of communication tester or BS emulator, fading emulator and anechoic chamber

with several OTA probes placed. The channel model affects the probe configurations. Since in 2D channel models the intended field to the wireless devices arrives on the horizontal plane, the probes are usually placed on the horizontal plane on a circle around the test zone. This case is referred to as the 2D case. If the range of possible multipath arrival elevation angles is limited around the horizon then the optimum probe locations would be a 'barrel' shaped configuration, which is referred to as 2.5D case. Furthermore, in 3D channel models where all elevation and azimuth angles are equally probable the probes need to be spread over a spherical surface. This case is referred to as the 3D case. As the intended fields (5.1) include both the vertical and horizontal components then both the vertically (θ) and horizontally (φ) polarized probes need to be employed.

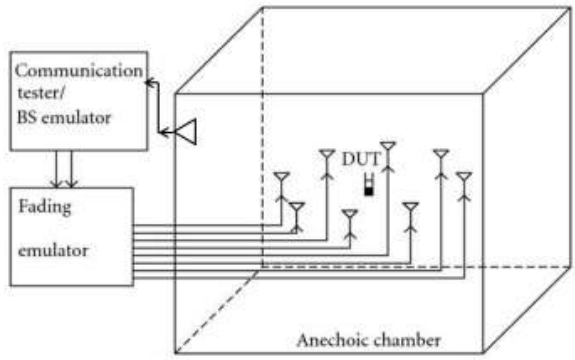

Figure 5.2. Illustration of a multi-probe MIMO OTA testing.

The DUT is in the center of the circular (2D case) or spherical (3D case) test zone. The communication tester receives an uplink signal from the DUT and also transmits the downlink signal, which is fed to the multichannel fading emulator. The fading emulator produces the multipath propagation channel. The output ports of the fading emulator are connected to the OTA probes. Typically, a power amplifier between a fading emulator output and a probe is required to adjust the power at the DUT. Generally, both downlink and uplink transmissions are required in MIMO OTA testing to get the final performance metric. The DUT forwards an uplink signal to the communication tester located outside the chamber. The uplink signal is once received by a communication antenna inside the chamber and then transferred to the communication tester via a coaxial cable. A proper communication antenna would be a circularly polarized antenna with high directivity.

5.4.2 Emulation techniques

Prefaded signal synthesis (PFS)

The PFS technique uses prefaded signals at each probe where the power-adjusted signals from the multi-probes are combined over the air to produce an accurate angular spread representation of the signal for each delay inside the test zone [66, 82]. The test zone is the geometrical volume inside which the DUT is located during the test. In PFS, the temporal dispersion of the desired channel is explicitly generated by the fading emulator instead of by the ever-changing superposition of a myriad of multipath components. The spatial dispersions of the channel model are mapped onto the multi-probes in such a way that the target spatial correlation functions can be synthesized. The accuracy metric of PFS technique is the root mean square (rms) error in spatial correlation function. The target is to find the optimum power weights of the OTA probes that minimize the rms error between the theoretical spatial correlation resulting from the target continuous APS and the synthesized spatial correlation resulting from discrete APS.

Plane-wave field synthesis (PWS)

With respect to PWS, two types of setup exist, one where the distances between OTA probes obey the Nyquist sampling criterion and other one where such criterion is not obeyed. The latter is typically the reciprocal of near-field antenna measurement setups (in analysis mode) or the real-time equivalent of the near-field setup working with virtual synthesis. The proposed multi-probe based OTA test setups in the literatures are of the latter type. Principally, irrespective of the two types, for synthesis, one should find those excitation voltages of the OTA probes that cause the superposition of the radiated fields to match the prescribed fields tangential to the surface of the test volume [21, 83].

For the first type of setups, the synthesis is done just by taking the components of the target field at the OTA probe positions tangential to the test surface by utilizing the Huygens' Principle. This is typically the approach studied in acoustic wave field synthesis and in [84].

For the second type of setups, almost invariably inversion, of the known fields generated by the OTA probe on the test zone surface, is used to derive the proper excitations for the OTA probes [83, 85-87, **VIII**]. The PWS reported in [85-86, **VIII**] is based on the synthesis of electromagnetic field environment using the spherical wave theory [21] whereas [83, 87] deal with PWS based on

a plane-wave description. In [87], the PWS is considered for purely 2D case with hypothetical line sources while regular OTA ring array is considered in [83].

Advantages and disadvantages

Of these two described techniques for emulating the field environment inside the test zone, an advantage of the PWS is that the PWS approach supports the emulation of any circumstances (e.g., angularly static or dynamic) of an arbitrary channel whereas PFS doesn't support modeling of LOS path with arbitrary AoA and thus not with dynamic LOS path direction neither [82]. Additionally, PWS supports controlled linear, circular, or elliptic polarization of the multipath. A drawback of the PWS is requirement of the phase calibration that is not needed in PFS.

In PWS technique using Huygens' Principle, the Huygens' sources are placed on the surface of the test volume and thus the required chamber will be small enough in size, which reduces the cost of the MIMO OTA test setup significantly. On the other hand, the mutual coupling between the sources will be increased for such a large number of sources placed on the test surfaces, resulting in increased measurement uncertainty and need of complex antenna calibration. Additionally, this method increase the system cost due to required number of coherent output channels of the fading emulator.

5.5 Contributions of this thesis

The contributions of this thesis with respect to multi-probe method for MIMO OTA testing are contained in publications [**V**–**VIII**]. The results of [**V**–**VIII**] add imperative aspects of multi-probe testing. It is of general interest among the mobile communications industry what are the uncertainties in the determination of the desired FoM with such a system, how can such systems be calibrated, how one can verify that the synthesized channel conditions do match with those of the channel model and how to compensate the near-field effect and range reflections. The research in this thesis is focused on clarifying some of these aspects in both theory and practice.

Publication [**V**], clarifies the very important and cost-related issue of the required number of probes for synthesizing the desired fields inside the multi-probe system. The synthesis technique utilized in [**V**] is the PWS based on spherical wave theory. According to this theory, any arbitrary electromagnetic fields can be described by means of SWE. This spherical wave theory offers

theoretical justification of the number of probes because of its well-known cut-off properties of the basis function. First, the well-known general rules for the number of probes as a function of the test zone size in wavelengths are presented for both 2D and 3D cases, and then accurate rules for the minimum number of required probes have been established taking into account the uncertainty level of the 2D field synthesis. In order to evaluate the accuracy of the PWS technique, the maximum relative error between the synthesized and intended field on the circumference of the test zone is evaluated which is called equivalent reflectivity level [85]. It is shown that the number of required probes for synthesizing the intended plane waves with a predefined accuracy is dictated by the radius of the test zone and not affected by the number of intended plane waves of the channel model.

In [**VI**], measurement uncertainties and limitations related to the use of the multi-probe system for reliable MIMO OTA testing are investigated against equivalent reflectivity level of the field synthesis. The topics related to the uncertainties include investigation of the required number of probes, optimum probe placement and the influence of the probe polarization. The investigation is carried out for particularly 2D multi-probe systems where WINNER II is chosen as a reference channel model to be synthesized. Nonetheless, any geometry-based channel model can be used. Computer simulations are performed where the radius of the probe circle is varied with different probe configurations. Two different probe configurations are analyzed, case 1: where probes are dual polarized at each location and case 2: where half of the probes are vertically polarized and half are horizontally polarized. The effect of probe placement error, i.e., probe location mismatch on the reflectivity level of the field synthesis is also studied.

In [**VII**], the probe configurations for emulating 2.5D and 3D channels are studied. Different 3D and 2.5D probe configurations for MIMO OTA testing of different DUT sizes are assessed where IMT-Advanced urban macro (UMa) NLOS with uniform azimuth PAS and Laplacian shaped elevation PAS is chosen as a representative channel. The selected model is expected to be the most difficult scenario to emulate as it has the widest angular spread in elevation and the highest asymmetry with respect to the horizon. This is confirmed in [82] that the synthesis accuracy decreased with the increasing angular spread of the PES of the channel model. Two criteria are used to evaluate the probe configuration: rms error in spatial correlation function using PFS and reflectivity level using PWS. Both criteria provide the similar recommendations for different test zone sizes.

In [**VIII**] verification of the emulation technique, PWS based on the spherical wave theory relevant to multi-probe based MIMO OTA testing is presented. A method of creating the desired channel condition using the limited number of probes is derived. A computer simulation platform is built firstly to verify the technique numerically, where WINNER II is chosen as a reference channel model. In the simulation, a 2×2 MIMO link is considered. An antenna array with two half-wave length electric dipoles is considered for both Tx and Rx antenna. The statistical properties of the emulated MIMO channel matrix using the multi-probe testing are compared with those of the reference MIMO channel matrix. The comparison is made in terms of the fading statistics, spatial and temporal correlation coefficients and channel capacity. The correlation coefficients and channel capacity are significant candidates FoMs in MIMO OTA testing. Simulation results show accuracy of the channel emulation using the PWS technique for the considered channel. Furthermore, the impact of number of probes on the accuracy of reproduced the channel capacity is also studied. Finally, the emulation technique is verified experimentally by examining the emulated field inside the test zone and MIMO throughput in a practical 2D multi-probe test facility. The results demonstrate feasibility and accuracy of the PWS technique for the considered case. For MIMO throughput evaluation a realistic DUT with good, nominal and bad reference antenna [88] is considered.

6. Summary of the publications

In publication [**I**], a new method is presented for generating the spherical mode responses of a channel requited in the spherical wave modeling of the radio channel. A natural scan surface for the direct spherical data extraction would be spherical. In [**I**], the required spherical mode responses of the channel are extracted from the measurement data acquired on a cubical scanning surface. Such data is easily obtainable with widely available 3D linear scanners. The field generation method from the cubical surface scanning is based on the spherical wave theory. The accuracy of the field generation is studied through simulations. Any type of probes can be applied with the proposed method.

Publication [**II**] deals with the improvement of the data extraction in cubical surface scanning. The post processing of the measured data required by the cubical surface scanning is computationally intense. A novel technique for the reduction of the computational burden is described in [**II**]. The reduction method is the azimuthal mode decomposition of the field responses. The method utilizes the orthogonal properties of the spherical wave functions. The method is applicable with a general probe as it is independent of the probe pattern used for cubical surface scanning.

In publication [**III**], the cubical surface scanning is investigated as a near-field measurement technique for finding the antennas coefficients for determining the far-field radiation pattern through the near-field to far-field transformation. The most important issue in [**III**] is to introduce the azimuthal mode decomposition technique to be applied as a part of the near-field to far-field transformation allowing a reduction in the computational burden of the transformation. The results show the applicability of cubical surface scanning for extracting the antenna coefficients and importantly the feasibility of the azimuthal mode decomposition technique in this context.

Publication [**IV**] presents a novel method for estimating the degrees of freedom of the multipath propagation channel. If this number can be established, it will give the maximum number of antenna elements that can meaningfully exploit the multipath richness for spatial multiplexing or diversity. Publication [**IV**] offers an antenna-independent assessment of the degrees of freedom. Method presented in [**I**] is applied to generate each single spherical wave modes as accurately as possible. The functionality of the method is demonstrated through measurements in an anechoic chamber. Acquiring the soundness of the method, the degrees of freedom of indoor multipath channels is analyzed. The results in [IV] have significance to both antenna and the radio communication research community.

The results in publications [**V**−**VIII**] add imperative aspects of multi-probe based MIMO OTA testing. In publications [**V**] and [**VI**], investigations on related uncertainties associated with multi-probe based MIMO OTA testing; particularly 2D multi-probe systems are done. The topics related to the uncertainties include investigation of the required number of probes, optimum probe placement and the influence of the probe polarization. The very important and cost related issue of the required number of probes for synthesizing the desired fields inside the multi-probe system is examined in [**V**]. The synthesis technique utilized in [**V**] is the plane-wave field synthesis based on the spherical wave expansion of the electromagnetic field. The errors in the synthesized field with respect to the number of probes in the system are investigated. The rules for the minimum number of required probes are established by taking into account the uncertainty level of the field synthesis. In publication [**VI**], optimum probe placement and the influence of the probe polarization in multi-probe based 2D MIMO OTA testing are examined using the plane-wave field synthesis technique. WINNER II is chosen as a reference channel model to be synthesized.

Publication [**VII**] deals with 3D and 2.5D probe configurations for MIMO OTA testing of different DUT sizes. IMT-Advanced channels extended to 3D are considered as a reference channel. The figure of merits of probe configurations are the rms error in spatial correlation function and the synthesis error calculated based on deviation between the target electric field and the synthesized field. The results show the similar recommendations for probe configurations for different DUT sizes using both figure of merits.

Publication [**VIII**] deals with simulation and measurement verifications of multi-probe based MIMO OTA testing where plane-wave field synthesis is used as an emulation technique. A simulation model for multi-probe based

MIMO OTA test setup is built where WINNER II is chosen as a reference channel model. Having confirmed the soundness of the plane-wave field synthesis technique by simulations and measurements, the throughputs of the MIMO devices are measured and compared with the simulated one. The results demonstrate feasibility and accuracy of the plane-wave field synthesis technique.

7. Conclusions

This thesis contributes to the development of methods to characterize the field environment of the propagation channel and the radiation of mobile terminals. The characterization is based on the spherical wave expansion of the fields, which provides the opportunity to obtain a compact and comprehensive description of the entire problem including the base station, the multipath propagation channel, and the mobile terminal with multiple antennas, improving the accuracy with respect to the use of the traditional plane-wave and far-field based modeling. Furthermore, the research in this thesis can be used to develop evaluation methods for the performance of the MIMO systems.

Theoretical considerations of the spherical wave expansion for the antenna array configuration on the cubical surface for estimating the propagation channel were studied in this thesis. Three orthogonal antenna polarizations were considered for determining the array configuration. It was shown that such a configuration was able to generate the spherical wave modes of the propagation channel. Guidelines for choosing the number of antenna elements of the array to generate spherical wave modes have been presented.

Furthermore, the antenna configuration on the cubical surface was investigated for the near-field antenna measurement and related near-field to far-field transformation. The results showed the benefits of this method. Nonetheless, using this method for field generation and near-field to far-field transformation, the subsequent data processing is computationally intense. In this thesis, a novel technique, azimuthal mode decomposition for the reduction of the computational burden was presented for both the applications and the results showed the feasibility of this technique. Interesting future work would be to examine techniques for further reducing the computational burden and lowering the computational complexity of the near-field to far-field transformation.

The proposed antenna configuration on the cubical surface with three orthogonal polarizations was investigated for the estimation of degrees of freedom in measured multipath channels with varying environmental conditions. In this work, the degrees of freedom has been derived by means of the spherical wave expansion of electromagnetic fields radiated from an antenna array on the cubical surface having a certain aperture size. The degrees of freedom provides the number of antenna elements on the aperture for efficient improvement of the system performance by utilizing the spatial transmission, e.g., diversity and multiplexing.

Furthermore, in this work the MIMO OTA testing has been discussed. In such testing, reproduction of radio channel environments in laboratory conditions is required. One possible way to synthesize radio channel environments is through the exploitation of multi-probe technology. Several practical aspects of multi-probe base MIMO OTA testing has been considered. First, a careful empirical study has been provided that shows the dependence of field synthesis error on the number of probes that are used to surround a device under test in an anechoic chamber. The results provide a way to obtain an accuracy parameter used with spherical wave functions in terms of a more available metric, equivalent reflectivity level. Second, a study on probe position error demonstrates that OTA methods are insensitive too small to moderate errors. Third, a study of a true OTA setup was developed and it is shown that system throughput performance in the MIMO OTA setup matches that of detailed simulations using the same channel model. Future tasks in the MIMO OTA testing include the evaluation of MIMO link performance in more realistic wireless environment including user effects and interference from different base stations.

Bibliography

[1] E. Dahlman, S. Parkvall, J. Skold, and P. Beming, *3G Evolution: HSPA and LTE for Mobile Broadband*. Academic Press, Elsevier, 2008.

[2] A. D. Yaghjian, "An overview of near-field antenna measurements," *IEEE Transaction on Antennas and Propagation*, vol. 34, no. 1, pp. 30-45, Jan. 1986.

[3] F. D'Agostino, F. Ferrara, C. Gennarelli, and G. Riccio, "Error filtering in NF-FF transformation with plane-polar scanning," In *Proceeding of the 17th International Conference on Applied Electromagnetics and Communications,* pp. 332-335, 1-3 Oct. 2003.

[4] S. F. Gregson, C. G. Parini, and J. Dupuy, "Probe corrected plane bi-polar near-field antenna measurements," In *Proceeding of the Second European Conference on Antenna and Propagation*, pp. 1-6, 11-16 Nov. 2007.

[5] A. A. Glazunov, M. Gustafsson, A. F. Molisch, and F. Tufvesson, "Physical modelling of multiple-input multiple-output antennas and channels by means of the spherical vector wave expansion," *IET Microwaves, Antennas and Propagation,* vol. 4, no. 6, pp. 778-791, June 2010.

[6] S. Sesia, I. Toufik, and M. Baker, *LTE-The UMTS Long Term Evolution*, John Wiley & Sons, Chichester, UK, 2nd edition, 2011.

[7] *Q. Li, X. Lin, J. Zhang, and W. Roh, "Advancement of MIMO technology in WiMAX: from IEEE 802.16d/e/j to 802.16m," IEEE Communication Magazine, vol. 47, no. 6, pp. 100–107, June 2009.*

[8] R. Vaughan and J. Andersen, "Antenna diversity in mobile communications," *IEEE Transaction on Vehicular Technology,* vol. 36, no. 4, pp. 149-172, Nov. 1987.

[9] M. Jensen and J. Wallace, "A review of antennas and propagation for MIMO wireless communications," *IEEE Transaction on Antennas and Propagation,* vol. 52, no. 11, pp. 2810-2824, Nov. 2004.

[10] A. Paulraj, D. Gore, R. Nabar, and H. Bolcskei, "An overview of MIMO communications - a key to gigabit wireless," *Proceedings of the IEEE*, vol. 92, no. 2, pp. 198-218, Feb. 2004.

[11] G. J. Foschini and M. J. Gans, "On limits of wireless communications in a fading environment when using multiple antennas," *Wireless Pers. Commun*., vol. 6, no. 3, pp. 311–335, Mar. 1998.

[12] B. K. Lau, MIMO: *From Theory to Implementation (Alain Sibille, and Claude Oestges, and Alberto Zanella).* Elsevier, 2011, Ch 10: Multiple Antenna Terminals.

[13] L. Zheng and D. N. C. Tse, "Diversity and multiplexing: a fundamental tradeoff in multiple-antenna channels," *IEEE Transaction on Information Theory*, vol. 49, no. 5, pp. 1073-1096, May 2003.

[14] 3GPP, Technical Specification Group Radio Access Network; Measurements of radio performances for UMTS terminals in speech mode (Release 7), June, 2006.

[15] Cellular Telecommunications & Internet Association (CTIA), "CTIA test plan for mobile station over the air performance, Revision 2.2," CTIA, Washington DC, Tech. Rep., Nov. 2006, 173 p.

[16] M. Landmann, M. Grossmann, N. Phatak, C. Schneider, R. Thomae, and G. Del Galdo, "Performance analysis of channel model simplifications for MIMO OTA LTE UE testing", In *Proceedings of the 7th European Conference on Antennas and Propagation (EuCAP 2013)*, pp. 1856 – 1860, 8-12 April 2013.

[17] H.-O. Ruoss, J. Christ, and F. M. Landstorfer, "Multiple probe nearfield scanning for EMC-investigations," In *Proceeding of the 27th European Microwave Conference,* vol. 1, pp. 556-560, 8-12 Sept. 1997.

[18] P. O. Iversen, P. Garreau, and D. Burrell, "Real-time spherical near-field handset antenna measurements," *IEEE Antennas and Propagation Magazine*, vol. 43, no. 3, pp. 90-94, June 2001.

[19] T. A. Laitinen, J. Ollikainen, C. Icheln, and P. Vainikainen, "Rapid spherical 3-D field measurement system for mobile terminal antennas," In *Proceeding of the Instrumentation and Measurement Technology Conference, IMTC '03,* vol. 2, pp. 968-972, 20-22 May 2003.

[20] R. C. Wallace, J. Bartlett, and J. K. M. Lee, "Method and apparatus for testing and evaluating wireless communication devices," U.S. Patent Application Publication, US 2003/0003883 A1, Jan. 2, 2003.

[21] J. E. Hansen, *Spherical Near-Field Antenna Measurements*. UK, London: Peter Peregrinus Ltd., 1988.

[22] S. L. Belousov, *Tabes of Normalized Associated Legendre Polynomials*, Pergamon Press, Oxford, 1962.

[23] T. Laitinen, "Advanced Spherical Antenna Measurements," Thesis for the degree of the Doctor of Science in Technology, TKK, Espoo, December, 2005.

[24] I. E. Telatar, "Capacity of multi-antenna Gaussian channels," *European Transactions on Telecommunications*, 10, November-December 1999.

[25] J. H. Winters, "On the capacity of radio communication systems with diversity in a Rayleigh fading environment," *IEEE Journal on Selected Areas in Communications,* vol. 5, no. 5, pp. 871-878, June 1987.

[26] M. Steinbauer, A. F. Molisch, and E. Bonek, "The double-directional radio channel," *IEEE Antennas and Propagation Magazine,* vol. 43, no. 4, pp. 51-63, Aug. 2001.

[27] 3GPP, Spatial channel model for MIMO simulations, TR 25.996 V6.1.0, 2003.

[28] D. S. Baum, J. Hansen, and J. Salo, "An interim channel model for beyond-3G systems: extending the 3GPP spatial channel model (SCM)," In *Proceeding of the 61st Vehicular Technology Conference, (VTC Spring 2005)*, vol. 5, pp. 3132-3136, 30 May-1 June 2005.

[29] 3GPP, E-UTRA MIMO channel model – text proposal, R1-061002.

[30] 3GPP, System level channel models for E-UTRA evaluations, R1-061594.

[31] 3GPP, Update of polarization description in link level channel model, R1-061371.

[32] IST-4-027756 WINNER II D1.1.1 WINNER II interim channel models, v1.0, December 2006.

[33] "Guidelines for evaluation of radio interface technologies for IMT Advanced, ITU-R Report M.2135," ITU-R, Tech. Rep., 2008.

[34] L. Liu, J. Poutanen, F. Quitin, K. Haneda, F. Tufvesson, P. D. Doncker, P. Vainikainen, and C. Oestges, "The COST2100 MIMO channel model," *IEEE Wireless Communications*, vol. 19, no. 6, pp. 92–99, December 2012.

[35] J. P. Kermoal, L. Schumacher, K. I. Pedersen, P. E. Mogensen, and F. Frederiksen, "A stochastic MIMO radio channel model with experimental validation," *IEEE Journal on Selected Areas in Communications,* vol. 20, no. 6, pp. 1211-1226, Aug. 2002.

[36] M. Gustafsson and S. Nordebo, "Characterization of MIMO antennas Using spherical vector waves," *IEEE Transactions on Antennas and Propagation,* vol. 54, no. 9, pp. 2679-2682, Sept. 2006.

[37] A. A. Glazunov, M. Gustafsson, A. F. Molisch, F. Tufvesson, and G. Kristensson, "Spherical vector wave expansion of Gaussian electromagnetic fields for antenna-channel interaction analysis," *IEEE Transactions on Antennas and Propagation,* vol. 57, no. 7, pp. 2055-2067, July 2009.

[38] Marzieh Dashti, "Time-of-Arrival estimation for UWB localizers in Indoor Multipath Environments", Ph.D thesis submitted to Department of International development engineering, Tokyo Institute of Technology, Tokyo, Japan, December 2011.

[39] K. Haneda, A. Khatun, C. Gustafson, and S. Wyney, "Spatial degrees-of-freedom of 60 GHz multiple-antenna channels," In *Proceeding of the 77th Vehicular Technology Conference (VTC Spring 2013)*, pp. 1-5, June 2013.

[40] K. Haneda, A. Khatun, V.-M. Kolmonen, and J. Salmi, "Dynamics of apatial degrees-of-freedom in MIMO mobile channels," In *Proceedings of the 7th European Conference on Antennas and Propagation (EuCAP 2013),* pp. 2801-2805, 8-12 April 2013.

[41] A. Khatun, T. Laitinen, and P. Vainikainen, "Spherical wave modelling of radio channels using linear scanners", in COST 2100 9th Management Committee Meeting, Sep. 28-30, 2009, Vienna, Austria, TD(09) 975.

[42] A. Khatun, T. Laitinen, and P. Vainikainen, "Noise sensitivity analysis of spherical wave modelling of radio channels using linear scanners," *Asia-Pacific Microwave Conference Proceedings (APMC 2010),* pp. 2119-2122, 7-10 Dec. 2010.

[43] C. H. Schmidt, T. A. Laitinen, and T. F. Eibert, "Fast Fourier Transform preprocessing for accelerated plane wave based spherical near-field far-field transformation," In *Proceedings of URSI International Symposium on Electromagnetic Theory (EMTS 2010)*, pp. 784-787, 16-19 Aug. 2010.

[44] J. Salo, P. Suvikunnas, H. M. El-Sallabi, and P. Vainikainen, "Ellipticity statistic as measure of MIMO multipath richness," *Electronics Letters*, vol. 42, no. 3, pp. 160-162, Feb. 2006.

[45] K. Nakai, J. Takada, M. Kim, D. Marzieh, and T. Laitinen, "Doubledirectional channel with the spherical harmonics," Tech. Rep. IEICE MW2009-198, Mar. 2010.

[46] A. A. Glazunov, M. Gustafsson, and A. F. Molisch, "On the physical limitations of the interaction of a spherical aperture and a random Field," *IEEE Transactions on Antennas and Propagation,* vol. 59, no. 1, pp. 119-128, Jan. 2011.

[47] A. S. Y. Poon, R. W. Brodersen, and D. N. C. Tse, "Degrees of freedom in multiple-antenna channels: a signal space approach," *IEEE Transactions on Information Theory,* vol. 51, no. 2, pp. 523-536, Feb. 2005.

[48] A. S. Y. Poon, D. N. C. Tse, and R. W. Broadersen, "Impact of scattering on the capacity, diversity, and propagation range of multiple-antenna channels," *IEEE Transactions on Information Theory,* vol. 52, no. 3, pp. 1087-1100, March 2006.

[49] J. Krogerus, P. Mäkikyrö, and P. Vainikainen, "Towards an applicable OTA test method for multi-antenna terminals," in COST 2100 6th Management Committee Meeting, Oct. 6-8, 2010, Lille, France, TD(08)671.

[50] http://www.3gpp.org/

[51] http://www.ctia.org/

[52] http://www.cost2100.org/

[53] 3GPP, "Technical specification group radio access network; measurements of radio performances for MIMO and multiantenna reception for HSPA and LTE terminals (Release 11)," May 2011.

[54] 3GPP, "Figure of merits for MIMO OTA measurements," May 2009.

[55] 3GPP, Technical Specification Group Radio Access Network; Evoloved Universal Terrestrial Radio Access (E-UTRA); User Equipment (UE) conformance specification Radio transmission and reception Part 1: Conformance Testing (Release 10)," Dec, 2011.

[56] Motorola, "UL-MIMO with antenna gain imbalance," 3GPP TSG RAN WG1, Ljubljana, Tech. Rep., Jan. 2009.

[57] W. C. Jakes, Microwave Mobile Communications. The Institute of Electrical and Electronics Engineers, NY, USA, 1974.

[58] G. J Foschini, "Layered space-time architecture for wireless communication in a fading environment when using multi-element antennas," *Bell Labs Tech J.*, pp. 41–59, 1996.

[59] C. A Balanis, *Antenna Theory, Analysis and Design*, New York, USA, 2nd Ed., J. Wiley Sons, 1997.

[60] T. Taga, "Analysis for mean effective gain of mobile antennas in land mobile radio environments," *IEEE Transactions on Vehicular Technology,* vol. 39, no. 2, pp. 117-131, May 1990.

[61] A. A. Glazunov, A. F. Molisch, and F. Tufvesson, "Mean effective gain of antennas in a wireless channel," *IET Microwaves, Antennas & Propagation,* vol. 3, no. 2, pp. 214-227, March 2009.

[62] P. Almers, E. Bonek, A. Burr, N. Czink, M. Debbah, V. Degli-Esposti, H. Hofstetter, P. Kyosti, D. Laurenson, G. Matz, A. Molisch, C. Oestges, and H. Oezcelik, "Survey of channel and radio propagation models for wireless MIMO systems," *EURASIP J. Wireless Commun. Networking*, 2007.

[63] P. Kyösti, J. Kolu, J.-P Nuutinen, M. Falck, and P. Mäkikyrö, "OTA testing for multiantenna terminals," in COST 2100 6th Management Committee Meeting, Oct. 6-8, 2010, Lille, France, TD(08)670.

[64] D. Kurita, Y. Okano, S. Nakamatsu, and T. Okada, "Experimental comparison of MIMO OTA testing methodologies," In *Proceedings of the 4th European Conference on Antennas and Propagation (EuCAP 2010),* pp. 1-5, 12-16 April 2010.

[65] A. Tankielun, E. Bohler, and C. von Gagern, "Two-Channel method for evaluation of MIMO OTA performance of wireless devices," in COST 2100 12th Management Committee Meeting, Nov. 23-25, 2010, Bologna, Italy, TD(10)046.

[66] W. Fan, X.C.B. de Lisbona, F. Sun, J.O. Nielsen, M.B. Knudsen, and G.F. Pedersen, "Emulating spatial characteristics of MIMO channels for OTA testing," *IEEE Transactions on Antennas and Propagation,* vol. 61, no. 8, pp. 4306-4314, Aug. 2013.

[67] L. J. Foged, A. Scannavini, N. Gross, and J. Estrada, "MIMO OTA testing using a multiprobe system approach," In *Proceedings of the 7th European Conference on Antennas and Propagation (EuCAP 2013),* pp. 1673-1677, 8-12 April 2013.

[68] 3GPP TS 34.114, "Discussion on some topical issues related to the spatial fading emulation based OTA test method for multi-antenna terminals", Nokia, February 2009.

[69] Elektrobit, "Updated Concept - MIMO OTA Testing," 3GPP TSG-RAN4 R4-092435 Seoul, Korea.

[70] Vodafone, Panasonic, Tokyo Institute of Technology, "MIMO OTA testing using RF controlled spatial fading emulator," R4-091390, 3GPP TSG RAN4 Meeting, 23rd – 27th March 2009, Seoul, Korea.

[71] W. Fan, X. Carreño, J. O. Nielsen, M. B. Knudsen, and G. F. Pedersen, "Verification of emulated channels in multi-probe based MIMO OTA testing setup," in *Proceedings of the 7th European Conference on Antennas and Propagation (EUCAP 2013),* pp. 97-101, 8-12 April 2013.

[72] Y. Okano, K. Kitao, and T. Imai, "Impact of number of probe antennas for MIMO OTA spatial channel emulator," in *Proceedings of the 3rd European*

Conference on Antenna and Propagation, (EuCAP 2010), pp. 1-5, 12-16 April 2010.

[73] W. Fan, F. Sun J. O. Nielsen, X. Carreno, J. S. Ashta, M. B. Knudsen, and G. F. Pedersen, "Probe selection in multiprobe OTA setups," *IEEE Transactions on Antennas and Propagation,* vol. 62, no. 4, pp. 2109-2120, April 2014.

[74] W. Fan, X. Carreño, J. Ø. Nielsen, K. Olesen, M. B. Knudsen, and G. F. Pedersen, "Measurement verification of plane wave synthesis technique based on multi-probe MIMO-OTA setup," in *Proceedings of the Vehicular Technology Conference (VTC Fall 2012),* pp. 1–5, 2012.

[75] W. Fan, I. Szini, M. D. Foegelle, J. O. Nielsen, and G. F. Pedersen, "Measurement uncertainty investigation in the multi-probe OTA setups," In Proceeding of the *8th European Conference on Antennas and Propagation (EuCAP 2014),* pp. 1068-1072, 6-11 April 2014.

[76] P. -S. Kildal and K. Rosengren, "Correlation and capacity of MIMO systems and mutual coupling, radiation efficiency, and diversity gain of their antennas: simulations and measurements in a reverberation chamber," *IEEE Communications Magazine,* vol. 42, no. 12, pp. 104-112, Dec. 2004.

[77] P.-S. Kildal, C. Orlenius, and J. Carlsson, "OTA testing in multipath of antennas and wireless devices with MIMO and OFDM," *Proceedings of the IEEE*, vol. 100, no. 7, pp. 2145-2157, July 2012.

[78] M. A. Garcia-Fernandez, J. D. Sanchez-Heredia, A. M. Martinez-Gonzalez, D. A. Sanchez-Hernandez, and J. F. Valenzuela-Valdes, "Advances in mode-stirred reverberation chambers for wireless communication performance evaluation," *IEEE Communications Magazine,* vol. 49, no. 7, pp. 140-147, July 2011.

[79] C. L. Patane, A. Skarbratt, R. Rehammar, and C. Orlenius, "On the use of reverberation chambers for assessment of MIMO OTA performance of wireless devices," In *Proceedings of the 7th European Conference on Antennas and Propagation (EuCAP 2013)*, pp. 101-105, 8-12 April 2013.

[80] Y. Jing Z. Wen, H. Kong, S. Duffy, and M. Rumney, "Two-stage over the air (OTA) test method for MIMO device performance evaluation," *IEEE International Symposium on Antennas and Propagation (APSURSI),* pp. 71-74, 3-8 July 2011.

[81] M. Rumney, H. Kong, and Y. Jing, "Practical active antenna evaluation using the two-stage MIMO OTA measurement method," In *Proceedings of*

the 8th European Conference on Antennas and Propagation (EuCAP 2014), pp. 1-5,6-11 April 2014.

[82] P. Kyösti, T. Jämsä, and J. Nuutinen, "Channel modelling for multiprobe over-the-air MIMO testing," International Journal of Antennas and Propagation, 2012, Article ID 615954, 11 pages.

[83] W. A. T. Kotterman, A. Heuberger, and R. Thoma, "*On the accuracy of synthesized wave-fields in MIMO-OTA set-ups*," in *Proceedings of the 5th European Conference on Antennas and Propagation (EUCAP 2011),* pp. 2560–2564, 11-15 April 2011.

[84] A. Khatun and K. Nikoskinen, "On the use of Huygens' sources for synthetic propagation environments with the application in MIMO over-the-air testing," *Progress in Electromagnetics Research Symposium (PIERS) Proceedings*, 621 - 624, August 12-15, Stockholm, 2013.

[85] T. Laitinen, P. Kyösti, J. Nuutinen, and P. Vainikainen, "On the number of OTA antenna elements for plane-wave synthesis in a MIMO OTA test system involving circular antenna array," In *Proceedings of the Forth European Conference on Antennas and Propagation (EuCAP 2010)*, pp. 1-5, 12-16 April 2010.

[86] J. Toivanen, T. Laitinen, V. Kolmonen, and P. Vainikainen, "Reproduction of arbitrary multipath environments in laboratory conditions," *IEEE Transactions on Instrumentation and Measurement,* vol. 60, no. 1, pp. 275-281, Jan. 2011.

[87] D. A. Hill, "A circular array for plane-wave synthesis," *IEEE Transaction on Electromagnetic Compatibility,* vol. 30, no. 1, pp. 3-8, February 1988.

[88] Motorola Mobility, "Reference antennas proposal for MIMO OTA", 3GPP TSG RAN WG4#59, R4-113032, Barcelona, Spain, May 2011.

Errata

Publication VI

In Section IV, p. 1382, δ is the standard deviation of the Normal or Gaussian distribution, not the error amplitude. The mean of the distribution is 6°.

The future mobile communications systems will provide increasing data rates to satisfy the service requirements of the users. This means that the radio performance of especially the mobile terminals becomes more important and has to be as good as possible. Thus, it is very important to be able to evaluate the performance of the antennas of the mobile terminals in a realistic way. This thesis deals with methods to characterize the field environment and the radiation of mobile terminals. The characterization is based on spherical wave expansion of the fields, which provides the opportunity to obtain a compact and comprehensive description of the entire problem including the base station, the multipath propagation channel, and the mobile terminal with multiple antennas to enhance the transfer capacity.

Aalto-DD 205/2014

ISBN 978-952-60-6009-5 (printed)
ISBN 978-952-60-6010-1 (pdf)
ISSN-L 1799-4934
ISSN 1799-4934 (printed)
ISSN 1799-4942 (pdf)

Aalto University
School of Electrical Engineering
Department of Radio Science and Engineering
www.aalto.fi

BUSINESS + ECONOMY

ART + DESIGN + ARCHITECTURE

SCIENCE + TECHNOLOGY

CROSSOVER

DOCTORAL DISSERTATIONS